Exploring the gauge flexibility of the linear-in-spin effective-one-body Hamiltonian at the 5.5 post-Newtonian order

Andrea Placidi,[1,*] Luca Sebastiani,[2,†] and Gianluca Grignani[1,‡]

[1]*Dipartimento di Fisica e Geologia, Università di Perugia, I.N.F.N. Sezione di Perugia, Via Pascoli, I-06123 Perugia, Italy*

[2]*Max Planck Institute for Gravitational Physics (Albert Einstein Institute), Am Mühlenberg 1, Potsdam 14476, Germany*

(Received 2 December 2025; accepted 12 March 2026; published 3 April 2026)

We derive the gauge-general expressions of the two gyro-gravitomagnetic functions entering the spin-orbit sector of the effective-one-body (EOB) Hamiltonian up to the fifth-and-half post-Newtonian (5.5PN) order. Our results include both local and nonlocal-in-time contributions, providing the most general analytical formulation of the linear-in-spin conservative dynamics within the EOB framework. These expressions are then employed to compute two gauge-invariant observables for quasicircular orbits: the binding energy and the fractional periastron advance. We also use them to compare two spin gauge choices: the well-known Damour-Jaranowski-Schäfer (DJS) gauge, in which the gyro-gravitomagnetic functions are independent of the orbital angular momentum, and the alternative anti-DJS (or $\overline{\text{DJS}}$) gauge, designed to reproduce in the test-mass limit the spin-orbit interaction of a spinning test particle in a Kerr background. For a circular, equal-mass, equal-spin binary, our analysis indicates that the $\overline{\text{DJS}}$ gauge provides a slightly improved description of the inspiral dynamics, suggesting potential advantages for its use in future EOB waveform models.

DOI: 10.1103/435y-8241

I. INTRODUCTION

The detection and detailed characterization of gravitational-wave (GW) signals from the coalescence of compact binaries are essential for inferring the properties of these systems, understanding their formation channels, and performing precise tests of general relativity (GR) [1–6]. Achieving these goals requires continually improving analytical waveform models. A key element of this modeling effort is the accurate description of spin effects in the orbital dynamics of compact binaries [7–36], as these effects leave a significant and observable imprint on the emitted gravitational radiation.

Several analytical approximation schemes have been developed to describe the conservative dynamics of compact binaries in GR. The post-Newtonian (PN) formalism [37–41] is an expansion valid in the slow-motion, large-separation (i.e., weak-field) regime and is typically organized as a series in inverse powers of the speed of light, where a term proportional to $1/c^n$ corresponds to the $\frac{n}{2}$PN order. The post-Minkowskian (PM) framework [42–45], by contrast, expands in the gravitational constant G and applies at arbitrary velocities while still requiring sufficiently large separations. Finally, the gravitational self-force (GSF) approach [46–49] relies on a perturbative expansion in the small mass ratio and is therefore restricted in mass range, while remaining valid in both strong-field and high-velocity regimes.

Building on one or more of these approximation schemes, the effective one-body (EOB) formalism [50–53] provides a powerful framework that (i) anchors the description of binary evolution to the strong-field dynamics of a test body, thereby extending the domain of validity of the underlying perturbative information, and (ii) consistently incorporates calibrations to numerical relativity (NR) simulations. The result is a semianalytical approach capable of generating accurate inspiral-merger-ringdown waveforms for coalescing binaries of any type, including systems with spin, tidal interactions, and eccentric orbits [54–81].

In the conservative sector, the EOB dynamics is typically encoded in a Hamiltonian

$$H_{\text{EOB}} = M\sqrt{1 + 2\nu(\hat{H}\text{eff} - 1)}, \tag{1}$$

*Contact author: andrea.placidi7@gmail.com
†Contact author: luca.sebastiani@aei.mpg.de
‡Contact author: gianluca.grignani@unipg.it

where the rescaled effective Hamiltonian $\hat{H}\text{eff} \equiv H_{\text{eff}}/\mu$ governs the motion in the effective problem associated with a binary system of total mass $M = m_1 + m_2$, reduced mass $\mu = m_1 m_2/M$, and symmetric mass ratio $\nu = \mu/M$. Neglecting contributions beyond linear order in the spins and considering spin-aligned (or antialigned) binaries, $\hat{H}_{\text{eff}}$ can be decomposed as [82]

$$\hat{H}_{\text{eff}} = \hat{H}^{\text{orb}}_{\text{eff}}(R, P_\varphi, P_R) + P_\varphi[G_S(R, P_\varphi, P_R)S + G_{S_*}(R, P_\varphi, P_R)S_*], \tag{2}$$

where R is the relative separation between the two bodies, P_φ is the orbital angular momentum, P_R is the radial momentum, and (S, S_*) denote the magnitudes of the linear combinations of the individual spins $(\mathbf{S}_1, \mathbf{S}_2)$ defined below in Eq. (5). In the decomposition (2), the orbital Hamiltonian $\hat{H}^{\text{orb}}_{\text{eff}}$, describing the nonspinning component of the conservative dynamics, is augmented by a spin-orbit term (second line) whose coupling strength is encoded in the two effective gyro-gravitomagnetic functions G_S and G_{S_*}.

Within the EOB framework, the functions G_S and G_{S_*} are fixed by matching the linear-in-spin results for the conservative two-body dynamics, as derived in any of the standard perturbative approaches. For instance, Refs. [74,83] determine them using PM-gravity results. In this work, instead, we focus on their determination within PN theory, whose linear-in-spin sector has been systematically developed across numerous studies.

In particular, Ref. [82] derived G_S and G_{S_*} at next-to-leading order, corresponding to 2.5PN accuracy in the Hamiltonian, a result later extended to 3.5PN in Refs. [84,85], and confirmed by an independent derivation in Ref. [86,87], using an effective-field-theory approach. By adapting the "Tutti Frutti" method [88–91] to spinning systems, Refs. [92,93] further determined G_S and G_{S_*} at 4.5PN order. More recently, the same strategy was employed in Ref. [94] to push the accuracy to 5.5PN.

It is important to recall that the explicit form of G_S and G_{S_*} is, in general, influenced by arbitrary choices of spin gauge. In Ref. [82], this freedom was used to impose the simplifying condition that both functions be independent of the angular momentum P_φ, thereby defining what is now known as the Damour-Jaranowski-Schäfer (DJS) gauge. While Refs. [84,85] computed G_S and G_{S_*} in a general, gauge-unfixed form, the higher-PN-order results of Refs. [92–94] were obtained exclusively in the DJS gauge. This motivated the recent analysis of Ref. [95], which derived the 4.5PN-accurate, gauge-unfixed expressions of G_S and G_{S_*} and carried out a first exploratory investigation of the potential advantages of adopting a spin gauge alternative to the DJS one, namely the so-called "anti-DJS" (or $\overline{\text{DJS}}$) gauge.

Prompted also by Ref. [96], which highlighted the benefits of the $\overline{\text{DJS}}$ gauge in the large-mass-ratio region of the parameter space, in the present work we extend the analysis of Ref. [95] by (i) pushing the gauge-general determination of the gyro-gravitomagnetic functions up to 5.5PN order, matching the accuracy of the DJS-gauge computation of Ref. [94], and (ii) providing the correspondingly accurate result within the $\overline{\text{DJS}}$ gauge. We then assess the performance of the two spin gauges by comparing the associated linear-in-spin binding energy for circular orbits.

As already shown in Ref. [94], tail-transported nonlocal-in-time terms appear in the 5.5PN spin-orbit sector of the conservative dynamics, just as they do in the orbital sector at 4PN order. We therefore follow the standard strategy of treating the local-in-time and nonlocal-in-time effects separately. At the level of the gyro-gravitomagnetic functions, this corresponds to the 5.5PN decomposition

$$G_S^{5.5\text{ PN}} = G_S^{5.5\text{ PN,loc}} + G_S^{5.5\text{ PN,nonloc}}, \tag{3a}$$

$$G_{S_*}^{5.5\text{ PN}} = G_{S_*}^{5.5\text{ PN,loc}} + G_{S_*}^{5.5\text{ PN,nonloc}}, \tag{3b}$$

where the local and nonlocal components, denoted respectively by the superscripts "loc" and "nonloc," are computed and provided separately.

Regarding the structure of the paper, we organize it as follows. In Sec. II, we clarify our notation and conventions. In Sec. III, we address the nonlocal contributions arising from tail effects, implementing the Delaunay-averaging procedure at 5.5PN order. This is complemented in Sec. IV by the derivation of the local-in-time component of the gyro-gravitomagnetic functions, which proceeds through the computation of the conservative, local-in-time part of the PN-expanded scattering angle. Section V is dedicated to the computation of the binding energy and periastron advance for quasicircular orbits, which also serve as diagnostic tools to test the 5.5PN-accurate, gauge-general expressions for G_S and G_{S_*} obtained in the previous sections. These expressions are then employed in Sec. VI to derive the corresponding forms in the DJS and $\overline{\text{DJS}}$ spin gauges, which we compare at the level of the spin-orbit contribution to the circular-orbit binding energy. Finally, we draw our conclusions in Sec. VII.

We also supplement this paper with an Appendix, which reviews additional technical details relevant to the computation discussed in Sec. III, and with a supplementary file [97], where we provide, in electronic form, all the main analytical results derived throughout this work.

II. COMPUTATIONAL SETUP

We consider a system of two Kerr black holes with masses m_1 and m_2, total mass $M = m_1 + m_2$, and reduced mass $\mu = m_1 m_2/(m_1 + m_2)$. Let ν denote the symmetric mass ratio and δ the antisymmetric mass ratio, defined as

$$\nu = \frac{\mu}{M}, \qquad \delta = \frac{m_1 - m_2}{M} = \sqrt{1 - 4\nu}, \tag{4}$$

where, without loss of generality, we assume $m_1 \geq m_2$.

Let $\mathbf{S}_1$ and $\mathbf{S}_2$ denote the spins of the two black holes. In the EOB description of spinning binaries, the basic spin variables are: the Kerr parameters $\mathbf{a}_i = \mathbf{S}_i/m_i$; the dimensionless spins $\chi_i = |\mathbf{S}_i|/m_i^2$; the effective linear combinations

$$\mathbf{S} = \mathbf{S}_1 + \mathbf{S}_2, \qquad \mathbf{S}_* = \frac{m_2}{m_1}\mathbf{S}_1 + \frac{m_1}{m_2}\mathbf{S}_2; \tag{5}$$

the symmetric and antisymmetric dimensionless spin combinations

$$\chi_S = \frac{\chi_1 + \chi_2}{2}, \qquad \chi_A = \frac{\chi_1 - \chi_2}{2}. \tag{6}$$

When referring to the nonrescaled, dimensionful quantities, the relative separation, angular momentum, radial momentum, and Hamiltonian are denoted by (R, P_R, P_φ, H). In the rescaled, dimensionless form, these variables are

$$r = \frac{R}{M}, \qquad p_r = \frac{P_R}{\mu}, \qquad p_\varphi = \frac{P_\varphi}{\mu M}, \qquad \hat{H} = \frac{H}{\mu}. \tag{7}$$

The rescaled total momentum is, as usual, given by $p^2 = p_r^2 + p_\varphi^2/r^2$. It is also convenient to introduce the dimensionless variable $u \equiv 1/r$, which, in geometric units, coincides with the magnitude of the Newtonian potential. Finally, for the gyro-gravitomagnetic functions we employ the u-rescaled combinations, $g_S \equiv G_S/u^3$ and $g_{S_*} \equiv G_{S_*}/u^3$.

In all our calculations, we restrict ourselves, for simplicity, to the case of spin-aligned (or antialigned) binaries. However, our results remain valid for generic precessing-spin configurations [92], since at linear order in the spins the gravitational spin-orbit coupling depends only on the scalar product between the spin and the orbital angular momentum, and is therefore insensitive to transverse spin components.

Because we focus exclusively on linear-in-spin effects, all higher-order spin contributions to the conservative dynamics are neglected throughout this work.

Finally, we adopt geometric units and set $G = c = 1$, restoring factors of $1/c$ only when needed to indicate the post-Newtonian order of PN-expanded expressions.

III. NONLOCAL SPIN-ORBIT DYNAMICS IN FULL GAUGE GENERALITY AT 5.5PN

In this section, we focus on the nonlocal 5.5PN components of the spin-orbit dynamics. We begin by recalling the procedure for computing the Delaunay-averaged Hamiltonian at 5.5PN accuracy. We then show how to use it, combined with a suitable general ansatz in the nonlocal spin-orbit part of the effective Hamiltonian, to determine the gauge-general expressions of $g_S^{5.5\,\mathrm{PN,nonloc}} = G_S^{5.5\,\mathrm{PN,nonloc}}/u^3$ and $g_{S_*}^{5.5\,\mathrm{PN,nonloc}} = G_{S_*}^{5.5\,\mathrm{PN,nonloc}}/u^3$, namely the nonlocal components of the 5.5PN gyro-gravitomagnetic functions introduced in Eq. (3).

A. Delaunay-averaged nonlocal Hamiltonian at 5.5PN

For the sake of clarity and self-consistency, we begin by briefly reviewing the computation of the 5.5PN Delaunay-averaged Hamiltonian, originally carried out in Ref. [94] and independently reproduced by us.

It is well known that, starting at the fourth subleading post-Newtonian order (namely at 4PN in the orbital sector and at 5.5PN in the spin-orbit sector), nonlocal-in-time contributions enter the conservative two-body dynamics. Accordingly, the action can be split into two components, $\mathcal{S}^{\mathrm{nPN}}_{\mathrm{tot}} = \mathcal{S}^{\mathrm{nPN}}_{\mathrm{loc}} + \mathcal{S}^{\mathrm{nPN}}_{\mathrm{nonloc}}$, where the orbital part of $\mathcal{S}^{\mathrm{nPN}}_{\mathrm{nonloc}}$ has been computed up to 6PN [53,89,91].

The nonlocal part of the rescaled action, containing the leading-order contributions in both the orbital and spin-orbit sectors (at 4PN and 5.5PN, respectively), is given by

$$\mathcal{S}^{\mathrm{LO}}_{\mathrm{nonloc}} = \int dt \mathrm{Pf}_{2s/c} \int \frac{dt'}{|t-t'|} \mathcal{F}^{\mathrm{sym}}_{\mathrm{LO}}(t,t'), \tag{8}$$

where $\mathrm{Pf}_{2s/c}$ denotes the Hadamard *partie finie* regularization [98] with arbitrary length scale s, introduced to regularize the singularity at $t' = t$, and $\mathcal{F}^{\mathrm{sym}}_{\mathrm{LO}}(t,t')$ is the time-symmetric gravitational-wave energy flux, restricted to its leading orbital and spin-orbit contributions.

Once the nonlocal action (8) is evaluated, the corresponding leading-order contribution to the Hamiltonian, denoted $\delta H^{\mathrm{LO}}_{\mathrm{nonloc}}$, follows directly from the nonlocal term in the action and is related to it through

$$\mathcal{S}^{\mathrm{LO}}_{\mathrm{nonloc}} = -\int dt \delta H^{\mathrm{LO}}_{\mathrm{nonloc}}(t). \tag{9}$$

To evaluate Eq. (8), we require the explicit form of the time-symmetric gravitational-wave energy flux,

$$\mathcal{F}^{\mathrm{sym}}_{\mathrm{LO}}(t,t') = \frac{1}{5} I^{(3)}_{ij}(t) I^{(3)}_{ij}(t') + \frac{16}{45c^2} J^{(3)}_{ij}(t) J^{(3)}_{ij}(t'), \tag{10}$$

where I_{ij} and J_{ij} denote the mass- and current-type quadrupole moments. Retaining only the leading-order contributions that are spin-independent or linear in the spins, their expressions in the center-of-mass frame read [99,100]

$$I_{ij} = M\nu x^{\langle i} x^{j\rangle} + \frac{1}{3c^3}\left[\frac{m_2^2}{M^2}(4v^{\langle i}(\mathbf{S}_1 \times \boldsymbol{x})^{j\rangle} - 5x^{\langle i}(\mathbf{S}_1 \times \boldsymbol{v})^{j\rangle}) + 1 \leftrightarrow 2\right], \tag{11a}$$

$$J_{ij} = M\delta\nu x^{\langle i}(\boldsymbol{x} \times \boldsymbol{v})^{j\rangle} + \frac{3}{2c}\left[\frac{m_2}{M} x^{\langle i} S_1^{j\rangle} - \frac{m_1}{M} x^{\langle i} S_2^{j\rangle}\right], \tag{11b}$$

where $\boldsymbol{x}$ and $\boldsymbol{v}$ denote the relative position and velocity of the binary, and angular brackets indicate the symmetric trace-free projection.

For the spin-aligned binaries we consider, the motion is planar. We can thus write

$$\boldsymbol{x} = Mr(\cos\varphi, \sin\varphi, 0), \tag{12a}$$

$$\boldsymbol{v} = M\dot{r}(\cos\varphi, \sin\varphi, 0) + Mr\dot{\varphi}(-\sin\varphi, \cos\varphi, 0), \tag{12b}$$

where we used mass-rescaled polar coordinates. It is then convenient to express r and φ in terms of orbital elements through the quasi-Keplerian parametrization, originally developed in Ref. [101], extended to 3PN accuracy in Ref. [102], and later generalized to include linear- and quadratic-in-spin contributions in Refs. [103,104]. At 1PN, the order we need in Eq. (8), such parametrization is given by

$$r = a_r(1 - e_r \cos u_e), \tag{13a}$$

$$\varphi = 2K \arctan\left[\sqrt{\frac{1+e_\varphi}{1-e_\varphi}} \tan\frac{u_e}{2}\right], \tag{13b}$$

$$\ell = nt = u_e - e_t \sin u_e, \tag{13c}$$

where a_r is the semimajor axis, e_r, e_φ, and e_t denote respectively the radial, angular, and time eccentricities, u_e is the eccentric anomaly, n is the mean motion, and K is the fractional periastron advance. For completeness, additional details on the quasi-Keplerian parametrization, as well as the relations between the orbital elements and the corresponding gauge-invariant quantities (at leading nonspinning and linear-in-spin order), are provided in the Appendix.

When inserting the parametrization (13) into the quadrupole moments (11a)–(11b), one must carefully handle the time derivatives. Up to relative 2.5PN order, the orbital elements $(a_r, e_r, e_\varphi, e_t, n, K)$ may be treated as constant in time, since each of them can be expressed in terms of energy and angular momentum [see Eqs. (A8)–(A15b)], which are conserved quantities before radiation-reaction effects enter at 2.5PN order [101,105].

Because the quasi-Keplerian parametrization is required here only up to 1.5PN accuracy, the eccentric anomaly u_e is the only remaining time-dependent variable, and its evolution is governed by Kepler's equation (13c), which yields

$$\dot{u}_e = \frac{n}{1 - e_t \cos u_e}. \tag{14}$$

This relation allows one to straightforwardly order-reduce the time derivatives appearing in the quadrupole moments.

It is important to remark that the integral (8) can only be analytically computed, for bound systems, within a small-eccentricity expansion. This is achieved by expressing the eccentricities e_r and e_φ in terms of e_t (see the Appendix) and then expanding in powers of e_t. In parallel, it is convenient to make the time dependence of u_e explicit by solving Kepler's equation in terms of Fourier-Bessel functions, namely

$$u_e = nt + \sum_{k=1}^{\infty} \frac{2}{k} J_k(ke_t) \sin(knt), \tag{15}$$

where the Fourier series can be truncated consistently at the same order as the eccentricity expansion.

Once these operations are carried out on the energy flux in Eq. (8), the Delaunay-averaged nonlocal Hamiltonian is obtained, as a function of a_r and e_t, by averaging over one orbital period.[1] In particular, by truncating the expansion in e_t at eighth order, we exactly reproduce the Delaunay-averaged Hamiltonian $\langle \delta H^{\rm LO}_{\rm nonloc} \rangle$ given in Eq. (2.19) of Ref. [94].

B. Nonlocal Delaunay-averaged EOB Hamiltonian at 5.5PN

The next step is to apply the Delaunay-averaging procedure at the level of the EOB Hamiltonian. Rewriting Eq. (1) in mass-rescaled form, we obtain

$$\hat{H}_{\rm EOB} = \frac{1}{\nu}\sqrt{1 + 2\nu(\hat{H}_{\rm eff} - 1)}, \tag{16}$$

where

$$\hat{H}_{\rm eff} = \sqrt{A(u)[1 + p^2 + (A(u)\bar{D}(u) - 1)p_r^2 + Q(u, p_r)]} + \frac{u^3 p_\varphi}{c^3}[g_S(u, p_r, p)S + g_{S_*}(u, p_r, p)S_*]. \tag{17}$$

For our purposes, the EOB potentials $A(u)$, $\bar{D}(u)$, and $Q(u, p_r)$ are taken at 4PN accuracy, including both their local and nonlocal parts. Among these, only the Q potential requires an eccentricity truncation; we implement this by retaining terms up to eighth order in the eccentricity, which corresponds to keeping powers of p_r up to p_r^8. For completeness, we report their explicit expressions as follows:

$$A(u) = 1 - 2u + a_3 u^3 + a_4 u^4 + (a_5^c + a_5^{\log} \log u)u^5, \tag{18a}$$

$$\bar{D}(u) = 1 + \bar{d}_2 u^2 + \bar{d}_3 u^3 + (\bar{d}_4^c + \bar{d}_4^{\log} \log u)u^4, \tag{18b}$$

$$Q(u, p_r) = q_{42} p_r^4 u^2 + q_{43} p_r^4 u^3 + q_{62} p_r^6 u^2 + q_{81} p_r^8 u, \tag{18c}$$

[1] This averaging procedure generates divergent integrals, which can be regularized, at this order, by taking their Hadamard *partie finie*; see, e.g., Sec. IV of Ref. [106] for further details on this regularization scheme.

where the coefficients read [53,89]

$$a_3 = 2\nu, \qquad a_4 = \left(\frac{94}{3} - \frac{41\pi^2}{32}\right)\nu, \qquad a_5^{\log} = \frac{64}{5}\nu, \tag{19a}$$

$$a_5^c = \left(\frac{2275\pi^2}{512} - \frac{4237}{60} + \frac{128}{5}\gamma_{\rm E} + \frac{256}{5}\ln 2\right)\nu + \left(\frac{41\pi^2}{32} - \frac{221}{6}\right)\nu^2, \tag{19b}$$

$$\bar{d}_2 = 6\nu, \qquad \bar{d}_3 = 52\nu - 6\nu^2, \qquad \bar{d}_4^{\log} = \frac{592}{15}\nu, \tag{19c}$$

$$\bar{d}_4^c = \left(-\frac{533}{45} - \frac{23761\pi^2}{1536} + \frac{1184}{15}\gamma_{\rm E} - \frac{6496}{15}\ln 2 + \frac{2916}{5}\ln 3\right)\nu + \left(\frac{123\pi^2}{16} - 260\right)\nu^2, \tag{19d}$$

$$q_{42} = 2(4 - 3\nu)\nu, \tag{19e}$$

$$q_{43} = \left(-\frac{5308}{15} + \frac{496\,256}{45}\ln 2 - \frac{33\,048}{5}\ln 3\right)\nu - 83\nu^2 + 10\nu^3, \tag{19f}$$

$$q_{62} = \left(-\frac{827}{3} - \frac{2\,358\,912}{25}\ln 2 + \frac{1\,399\,437}{50}\ln 3 + \frac{390\,625}{18}\ln 5\right)\nu - \frac{27}{5}\nu^2 + 6\nu^3, \tag{19g}$$

$$q_{81} = \left(-\frac{35\,772}{175} + \frac{21\,668\,992}{45}\ln 2 + \frac{6\,591\,861}{350}\ln 3 - \frac{27\,734\,375}{126}\ln 5\right)\nu. \tag{19h}$$

To single out the nonlocal component of the effective Hamiltonian, each EOB potential, as well as the two gyro-gravitomagnetic functions, is split into a local and a nonlocal contribution, as in Eq. (3).[2] Treating the nonlocal parts as small corrections (entering at 4PN in the potentials and at 5.5PN in g_S and g_{S_*}), we arrive at the following leading-order nonlocal contribution to the effective Hamiltonian:

$$\delta\hat{H}_{\rm eff}^{\rm nonloc} = \frac{1}{2}\left(A^{\rm nonloc} + \bar{D}^{\rm nonloc}p_r^2 + Q^{\rm nonloc}\right) + \frac{p_\varphi u^3}{c^3}\left[S g_S^{\rm 5.5PN,nonloc} + S_* g_{S_*}^{\rm 5.5PN,nonloc}\right]. \tag{20}$$

Since our goal is to derive fully general expressions for g_S and g_{S_*}, without imposing any *a priori* spin-gauge choice, we begin by introducing a general ansatz for their nonlocal 5.5PN components, to be inserted into Eq. (20). Focusing, for example, on g_S, the most general ansatz for its nonlocal part that is simultaneously compatible with the 5.5PN order and with the eighth order in eccentricity can be written as

$$\begin{aligned} g_S^{\rm 5.5PN,nonloc} = \frac{1}{c^8}\Bigg[& g_1^{\rm N^4LO,nl}u^4 + g_2^{\rm N^4LO,nl}p_r^2u^3 + g_3^{\rm N^4LO,nl}\dot{p}_r^2 + g_4^{\rm N^4LO,nl}p_r^4u^2 + g_5^{\rm N^4LO,nl}\frac{p_r^2\dot{p}_r^2}{u} + g_6^{\rm N^4LO,nl}\frac{\dot{p}_r^4}{u^4} \\ & + g_7^{\rm N^4LO,nl}p_r^6u + g_8^{\rm N^4LO,nl}\frac{p_r^4\dot{p}_r^2}{u^2} + g_9^{\rm N^4LO,nl}\frac{p_r^2\dot{p}_r^4}{u^5} + g_{10}^{\rm N^4LO,nl}\frac{\dot{p}_r^6}{u^8} + g_{11}^{\rm N^4LO,nl}p_r^8 + g_{12}^{\rm N^4LO,nl}\frac{p_r^6\dot{p}_r^2}{u^3} \\ & + g_{13}^{\rm N^4LO,nl}\frac{p_r^4\dot{p}_r^4}{u^6} + g_{14}^{\rm N^4LO,nl}\frac{p_r^2\dot{p}_r^6}{u^9} + g_{15}^{\rm N^4LO,nl}\frac{\dot{p}_r^8}{u^{12}} \\ & + \Bigg(g_{1,\log}^{\rm N^4LO,nl}u^4 + g_{2,\log}^{\rm N^4LO,nl}p_r^2u^3 + g_{3,\log}^{\rm N^4LO,nl}\dot{p}_r^2 + g_{4,\log}^{\rm N^4LO,nl}p_r^4u^2 + g_{5,\log}^{\rm N^4LO,nl}\frac{p_r^2\dot{p}_r^2}{u} + g_{6,\log}^{\rm N^4LO,nl}\frac{\dot{p}_r^4}{u^4} \\ & + g_{7,\log}^{\rm N^4LO,nl}p_r^6u + g_{8,\log}^{\rm N^4LO,nl}\frac{p_r^4\dot{p}_r^2}{u^2} + g_{9,\log}^{\rm N^4LO,nl}\frac{p_r^2\dot{p}_r^4}{u^5} + g_{10,\log}^{\rm N^4LO,nl}\frac{\dot{p}_r^6}{u^8} + g_{11,\log}^{\rm N^4LO,nl}p_r^8 + g_{12,\log}^{\rm N^4LO,nl}\frac{p_r^6\dot{p}_r^2}{u^3} \\ & + g_{13,\log}^{\rm N^4LO,nl}\frac{p_r^4\dot{p}_r^4}{u^6} + g_{14,\log}^{\rm N^4LO,nl}\frac{p_r^2\dot{p}_r^6}{u^9} + g_{15,\log}^{\rm N^4LO,nl}\frac{\dot{p}_r^8}{u^{12}}\Bigg)\log u\Bigg], \end{aligned} \tag{21}$$

where $(g_n^{\rm N^4LO,nl}, g_{n,\log}^{\rm N^4LO,nl})$ form a set of 30ν-dependent dimensionless coefficients. An analogous ansatz, involving another set of 30 coefficients $(g_{*n}^{\rm N^4LO,nl}, g_{*n,\log}^{\rm N^4LO,nl})$, is introduced for $g_{S_*}^{\rm 5.5PN,nonloc}$.

We remark that we have chosen the dynamical variables $(u, p_r, \dot{p}_r)$ in place of the more natural set (u, p_r, p^2), with $p^2 = p_r^2 + p_\varphi^2u^2$. This choice is motivated by the small-eccentricity expansion: our variables must also behave as consistent power counters in e_t. While $u = \mathcal{O}(e_t^0)$ and $p_r = \mathcal{O}(e_t) = \dot{p}_r$, the eccentricity counting is less transparent when using p.

[2]This type of local/nonlocal decomposition was first introduced in Ref. [106].

Nevertheless, once the matching is performed, one may always convert $\dot{p}_r$ back to p^2 by inverting the EOB Hamilton equation for p_r at the required PN accuracy.

Finally, the inclusion of logarithmic terms in the ansatz is necessary because, at the same PN order, the Delaunay-averaged nonlocal Hamiltonian obtained in the previous section contains contributions proportional to $\log a_r$.

After inserting the ansatz into $\delta\hat{H}^{\rm nonloc}_{\rm eff}$, the next step is to perform the Delaunay averaging. To this end, we use in Eq. (20) the Newtonian relations

$$p_r = \dot{r}, \qquad p_\varphi = r^2\dot{\varphi}, \qquad \dot{p}_r = \frac{r^3\dot{\varphi}^2 - 1}{r^2}, \quad (22)$$

and rewrite $\dot{r}$, r, and $\dot{\varphi}$ in terms of their quasi-Keplerian parametrization (13a)–(13c). No canonical transformation is needed here, since harmonic and EOB coordinates start to differ only at 2PN order.

We observe that this procedure yields two distinct sources of contributions to the nonlocal spin-orbit Hamiltonian at 5.5PN:

(i) a contribution originating from the 1.5PN (linear-in-spin) terms of the quasi-Keplerian parametrization, when these are applied to the nonlocal 4PN component of the EOB potentials;
(ii) a contribution arising directly from the nonlocal spin-orbit part of the Hamiltonian itself, for which, being already of 5.5PN order, it is sufficient to employ the Keplerian parametrization.

Expanding in eccentricity up to $\mathcal{O}(e_t^8)$ and performing the orbital average, we finally obtain the explicit expression of the 5.5PN nonlocal effective Delaunay Hamiltonian $\langle\delta H^{\rm LO}_{\rm eff,nonloc}\rangle$. The complete result is provided in electronic form in the Supplemental Materials accompanying this paper [97].

C. Nonlocal gyro-gravitomagnetic functions in full gauge generality at 5.5PN

By PN-expanding the energy map (16) and explicitly separating its local and nonlocal contributions, it is straightforward to verify that, at leading nonlocal order, one simply has $\delta H^{\rm LO}_{\rm EOB,nonloc} = \delta H^{\rm LO}_{\rm eff,nonloc}$.

We can thus partially fix the coefficients of our ansatz for $g_S^{\rm 5.5PN,nonloc}$ and $g_{S_*}^{\rm 5.5PN,nonloc}$ by directly identifying the two Delaunay-averaged Hamiltonians,

$$\langle\delta H^{\rm LO}_{\rm nonloc}\rangle = \langle\delta H^{\rm LO}_{\rm eff,nonloc}\rangle. \quad (23)$$

More precisely, the 5.5PN linear-in-spin sector of Eq. (23) yields 10 equations involving the 30 coefficients of $g_S^{\rm 5.5PN,nonloc}$, and an additional 10 equations involving the corresponding 30 coefficients of $g_{S_*}^{\rm 5.5PN,nonloc}$. Any solution of these two systems provides relations among the coefficients which, when substituted into the original ansatz, determine the gauge-unfixed expressions of the two gyro-gravitomagnetic functions. An explicit example of such a solution is provided in the Supplemental Materials [97].

Our result for the gauge-general expressions for the nonlocal 5.5PN components of g_S and g_{S_*} reads

$$\begin{aligned}
g_S^{\rm 5.5PN,nonloc} = {} & u^4\left[\nu\left(-\frac{64}{5}-\frac{1168}{15}\gamma_E-\frac{464}{3}\log 2\right)-\frac{584}{15}\nu\log u\right]+\dot{p}_r^2\left[-g_2^{\rm N^4LO,nl}+\nu\left(\frac{25\,564}{15}-208\gamma_E\right.\right.\\
& \left.+\frac{65\,488}{15}\log 2-\frac{23\,328}{5}\log 3\right)+(-104\nu+g_{2,\log}^{\rm N^4LO,nl})\log u\Big]+\frac{\dot{p}_r^4}{u^4}\left[8g_2^{\rm N^4LO,nl}-g_4^{\rm N^4LO,nl}-\frac{1}{3}g_5^{\rm N^4LO,nl}\right.\\
& -\frac{10}{3}g_{2,\log}^{\rm N^4LO,nl}+\nu\left(-\frac{58\,102}{5}+1664\gamma_E-\frac{7\,926\,272}{45}\log 2+124\,902\log 3\right)+\left(832\nu-8g_{2,\log}^{\rm N^4LO,nl}+g_{4,\log}^{\rm N^4LO,nl}\right.\\
& \left.+\frac{1}{3}g_{5,\log}^{\rm N^4LO,nl}\right)\log u\Big]+\frac{\dot{p}_r^6}{u^8}\left[-\frac{376}{5}g_2^{\rm N^4LO,nl}+\frac{47}{5}g_4^{\rm N^4LO,nl}+\frac{32}{15}g_5^{\rm N^4LO,nl}-g_7^{\rm N^4LO,nl}-\frac{1}{5}g_8^{\rm N^4LO,nl}-\frac{1}{5}g_9^{\rm N^4LO,nl}\right.\\
& +\frac{190}{3}g_{2,\log}^{\rm N^4LO,nl}-4g_{4,\log}^{\rm N^4LO,nl}-\frac{4}{5}g_{5,\log}^{\rm N^4LO,nl}+\nu\left(\frac{2\,724\,086}{25}-\frac{78\,208}{5}\gamma_E+\frac{80\,681\,472}{25}\log 2-\frac{8\,387\,631}{5}\log 3\right.\\
& \left.-\frac{3\,015\,625}{9}\log 5\right)+\left(-\frac{39\,104}{5}\nu+\frac{376}{5}g_{2,\log}^{\rm N^4LO,nl}-\frac{47}{5}g_{4,\log}^{\rm N^4LO,nl}-\frac{32}{15}g_{5,\log}^{\rm N^4LO,nl}+g_{7,\log}^{\rm N^4LO,nl}+\frac{1}{5}g_{8,\log}^{\rm N^4LO,nl}\right.\\
& \left.+\frac{1}{5}g_{9,\log}^{\rm N^4LO,nl}\right)\log u\Big]+p_r^8(g_{11}^{\rm N^4LO,nl}-g_{11,\log}^{\rm N^4LO,nl}\log u)+\frac{\dot{p}_r^8}{u^{12}}\left[712g_2^{\rm N^4LO,nl}-89g_4^{\rm N^4LO,nl}-\frac{416}{21}g_5^{\rm N^4LO,nl}\right.\\
& \left.+\frac{69}{7}g_7^{\rm N^4LO,nl}+\frac{61}{35}g_8^{\rm N^4LO,nl}+\frac{8}{7}g_9^{\rm N^4LO,nl}-g_{11}^{\rm N^4LO,nl}-\frac{1}{7}g_{12}^{\rm N^4LO,nl}-\frac{3}{35}g_{13}^{\rm N^4LO,nl}-\frac{1}{7}g_{14}^{\rm N^4LO,nl}-\frac{18\,982}{21}g_{2,\log}^{\rm N^4LO,nl}\right.
\end{aligned}$$

$$+\frac{1594}{21}g^{\mathrm{N^4LO,nl}}_{4,\log}+\frac{4964}{315}g^{\mathrm{N^4LO,nl}}_{5,\log}-\frac{30}{7}g^{\mathrm{N^4LO,nl}}_{7,\log}-\frac{24}{35}g^{\mathrm{N^4LO,nl}}_{8,\log}-\frac{2}{5}g^{\mathrm{N^4LO,nl}}_{9,\log}+\nu\bigg(-\frac{524\,132\,537}{525}+148\,096\gamma_E$$
$$-\frac{192\,215\,036\,288}{4725}\log 2+\frac{22\,292\,460\,117}{1400}\log 3+\frac{11\,346\,546\,875}{1512}\log 5\bigg)+\bigg(74\,048\nu-712g^{\mathrm{N^4LO,nl}}_{2,\log}+89g^{\mathrm{N^4LO,nl}}_{4,\log}$$
$$+\frac{416}{21}g^{\mathrm{N^4LO,nl}}_{5,\log}-\frac{69}{7}g^{\mathrm{N^4LO,nl}}_{7,\log}-\frac{61}{35}g^{\mathrm{N^4LO,nl}}_{8,\log}-\frac{8}{7}g^{\mathrm{N^4LO,nl}}_{9,\log}+g^{\mathrm{N^4LO,nl}}_{11,\log}+\frac{1}{7}g^{\mathrm{N^4LO,nl}}_{12,\log}+\frac{3}{35}g^{\mathrm{N^4LO,nl}}_{13,\log}+\frac{1}{7}g^{\mathrm{N^4LO,nl}}_{14,\log}\bigg)\log u\bigg]$$
$$+p_r^6\bigg[u(g_7^{\mathrm{N^4LO,nl}}-g^{\mathrm{N^4LO,nl}}_{7,\log}\log u)+\frac{\dot p_r^2}{u^3}(g_{12}^{\mathrm{N^4LO,nl}}-g^{\mathrm{N^4LO,nl}}_{12,\log}\log u)\bigg]+p_r^4\bigg[u^2(g_4^{\mathrm{N^4LO,nl}}-g^{\mathrm{N^4LO,nl}}_{4,\log}\log u)$$
$$+\frac{\dot p_r^2}{u^2}(g_8^{\mathrm{N^4LO,nl}}-g^{\mathrm{N^4LO,nl}}_{8,\log}\log u)+\frac{\dot p_r^4}{u^6}(g_{13}^{\mathrm{N^4LO,nl}}-g^{\mathrm{N^4LO,nl}}_{13,\log}\log u)\bigg]+p_r^2\bigg[u^3(g_2^{\mathrm{N^4LO,nl}}-g^{\mathrm{N^4LO,nl}}_{2,\log}\log u)$$
$$+\frac{\dot p_r^2}{u}(g_5^{\mathrm{N^4LO,nl}}-g^{\mathrm{N^4LO,nl}}_{5,\log}\log u)+\frac{\dot p_r^4}{u^5}(g_9^{\mathrm{N^4LO,nl}}-g^{\mathrm{N^4LO,nl}}_{9,\log}\log u)+\frac{\dot p_r^6}{u^9}(g_{14}^{\mathrm{N^4LO,nl}}-g^{\mathrm{N^4LO,nl}}_{14,\log}\log u)\bigg],\tag{24a}$$

$$g_{S_*}^{5.5\mathrm{PN,nonloc}}=u^4\bigg[\nu\bigg(-\frac{48}{5}-48\gamma_E-\frac{1456}{15}\log 2\bigg)-24\nu\log u\bigg]+p_r^8(g^{\mathrm{N^4LO,nl}}_{*11}-g^{\mathrm{N^4LO,nl}}_{*11,\log}\log u)$$
$$+\dot p_r^2\bigg[-g^{\mathrm{N^4LO,nl}}_{*2}+\nu\bigg(\frac{17\,512}{15}-\frac{512}{5}\gamma_E+\frac{46\,976}{15}\log 2-\frac{16\,038}{5}\log 3\bigg)+\bigg(-\frac{256}{5}\nu+g^{\mathrm{N^4LO,nl}}_{*2,\log}\bigg)\log u\bigg]$$
$$+\frac{\dot p_r^4}{u^4}\bigg[8g^{\mathrm{N^4LO,nl}}_{*2}-\frac{10}{3}g^{\mathrm{N^4LO,nl}}_{*2,\log}-g^{\mathrm{N^4LO,nl}}_{*4}-\frac{1}{3}g^{\mathrm{N^4LO,nl}}_{*5}+\nu\bigg(-\frac{123\,688}{15}+\frac{4096}{5}\gamma_E-\frac{373\,024}{3}\log 2+87\,480\log 3\bigg)$$
$$+\bigg(\frac{2048}{5}\nu-8g^{\mathrm{N^4LO,nl}}_{*2,\log}+g^{\mathrm{N^4LO,nl}}_{*4,\log}+\frac{1}{3}g^{\mathrm{N^4LO,nl}}_{*5,\log}\bigg)\log u\bigg]+\frac{\dot p_r^8}{u^{12}}\bigg[-g^{\mathrm{N^4LO,nl}}_{*11}-\frac{1}{7}g^{\mathrm{N^4LO,nl}}_{*12}-\frac{3}{35}g^{\mathrm{N^4LO,nl}}_{*13}-\frac{1}{7}g^{\mathrm{N^4LO,nl}}_{*14}$$
$$+712g^{\mathrm{N^4LO,nl}}_{*2}-\frac{18\,982}{21}g^{\mathrm{N^4LO,nl}}_{*2,\log}-89g^{\mathrm{N^4LO,nl}}_{*4}+\frac{1594}{21}g^{\mathrm{N^4LO,nl}}_{*4,\log}-\frac{416}{21}g^{\mathrm{N^4LO,nl}}_{*5}+\frac{4964}{315}g^{\mathrm{N^4LO,nl}}_{*5,\log}+\frac{69}{7}g^{\mathrm{N^4LO,nl}}_{*7}$$
$$-\frac{30}{7}g^{\mathrm{N^4LO,nl}}_{*7,\log}+\frac{61}{35}g^{\mathrm{N^4LO,nl}}_{*8}-\frac{24}{35}g^{\mathrm{N^4LO,nl}}_{*8,\log}+\frac{8}{7}g^{\mathrm{N^4LO,nl}}_{*9}-\frac{2}{5}g^{\mathrm{N^4LO,nl}}_{*9,\log}+\nu\bigg(-\frac{5\,043\,336}{7}+\frac{364\,544}{5}\gamma_E$$
$$-\frac{135\,717\,590\,272}{4725}\log 2+\frac{1\,576\,308\,681}{140}\log 3+\frac{3\,964\,671\,875}{756}\log 5\bigg)+\bigg(\frac{182\,272}{5}\nu+g^{\mathrm{N^4LO,nl}}_{*11,\log}+\frac{1}{7}g^{\mathrm{N^4LO,nl}}_{*12,\log}$$
$$+\frac{3}{35}g^{\mathrm{N^4LO,nl}}_{*13,\log}+\frac{1}{7}g^{\mathrm{N^4LO,nl}}_{*14,\log}-712g^{\mathrm{N^4LO,nl}}_{*2,\log}+89g^{\mathrm{N^4LO,nl}}_{*4,\log}+\frac{416}{21}g^{\mathrm{N^4LO,nl}}_{*5,\log}-\frac{69}{7}g^{\mathrm{N^4LO,nl}}_{*7,\log}-\frac{61}{35}g^{\mathrm{N^4LO,nl}}_{*8,\log}-\frac{8}{7}g^{\mathrm{N^4LO,nl}}_{*9,\log}\bigg)\log u\bigg]$$
$$+\frac{\dot p_r^6}{u^8}\bigg[-\frac{376}{5}g^{\mathrm{N^4LO,nl}}_{*2}+\frac{190}{3}g^{\mathrm{N^4LO,nl}}_{*2,\log}+\frac{47}{5}g^{\mathrm{N^4LO,nl}}_{*4}-4g^{\mathrm{N^4LO,nl}}_{*4,\log}+\frac{32}{15}g^{\mathrm{N^4LO,nl}}_{*5}-\frac{4}{5}g^{\mathrm{N^4LO,nl}}_{*5,\log}-g^{\mathrm{N^4LO,nl}}_{*7}-\frac{1}{5}g^{\mathrm{N^4LO,nl}}_{*8}$$
$$-\frac{1}{5}g^{\mathrm{N^4LO,nl}}_{*9}+\nu\bigg(\frac{5\,839\,172}{75}-\frac{192\,512}{25}\gamma_E+\frac{1\,537\,664\,096}{675}\log 2-\frac{5\,911\,461}{5}\log 3-\frac{6\,296\,875}{27}\log 5\bigg)$$
$$+\bigg(-\frac{96\,256}{25}\nu+\frac{376}{5}g^{\mathrm{N^4LO,nl}}_{*2,\log}-\frac{47}{5}g^{\mathrm{N^4LO,nl}}_{*4,\log}-\frac{32}{15}g^{\mathrm{N^4LO,nl}}_{*5,\log}+g^{\mathrm{N^4LO,nl}}_{*7,\log}+\frac{1}{5}g^{\mathrm{N^4LO,nl}}_{*8,\log}+\frac{1}{5}g^{\mathrm{N^4LO,nl}}_{*9,\log}\bigg)\log u\bigg]$$
$$+p_r^6\bigg[\frac{\dot p_r^2}{u^3}(g^{\mathrm{N^4LO,nl}}_{*12}-g^{\mathrm{N^4LO,nl}}_{*12,\log}\log u)+u(g^{\mathrm{N^4LO,nl}}_{*7}-g^{\mathrm{N^4LO,nl}}_{*7,\log}\log u)\bigg]+p_r^4\bigg[\frac{\dot p_r^4}{u^6}(g^{\mathrm{N^4LO,nl}}_{*13}-g^{\mathrm{N^4LO,nl}}_{*13,\log}\log u)$$
$$+u^2(g^{\mathrm{N^4LO,nl}}_{*4}-g^{\mathrm{N^4LO,nl}}_{*4,\log}\log u)+\frac{\dot p_r^2}{u^2}(g^{\mathrm{N^4LO,nl}}_{*8}-g^{\mathrm{N^4LO,nl}}_{*8,\log}\log u)\bigg]+p_r^2\bigg[\frac{\dot p_r^6}{u^9}(g^{\mathrm{N^4LO,nl}}_{*14}-g^{\mathrm{N^4LO,nl}}_{*14,\log}\log u)$$
$$+u^3(g^{\mathrm{N^4LO,nl}}_{*2}-g^{\mathrm{N^4LO,nl}}_{*2,\log}\log u)+\frac{\dot p_r^2}{u}(g^{\mathrm{N^4LO,nl}}_{*5}-g^{\mathrm{N^4LO,nl}}_{*5,\log}\log u)+\frac{\dot p_r^4}{u^5}(g^{\mathrm{N^4LO,nl}}_{*9}-g^{\mathrm{N^4LO,nl}}_{*9,\log}\log u)\bigg].\tag{24b}$$

The remaining coefficients in these expressions should be regarded as gauge coefficients, meaning that they do not affect physical observables, or more precisely, their determination at the 5.5PN order. By choosing their values appropriately, one can obtain the corresponding forms of $g_S^{5.5\mathrm{PN,nonloc}}$ and $g_{S_*}^{5.5\mathrm{PN,nonloc}}$ in any desired spin gauge.

IV. LOCAL SPIN-ORBIT DYNAMICS IN FULL GAUGE GENERALITY AT 5.5PN

We now turn to the local contribution to the 5.5PN conservative spin-orbit dynamics. Following Refs. [93–95], the physical quantity we work with in this case is the conservative scattering angle.

A. Conservative scattering angle: 5.5PN linear-in-spin terms

The scattering angle of a two-body gravitational system is a gauge-invariant quantity defined, in the context of unbound motion, as the deflection experienced by one body as a result of its interaction with the other. It is now well known that the conservative, local-in-time part of the scattering angle can be analytically continued from unbound to bound dynamics by replacing the scattering states with the corresponding bound states of the two-body system [107,108]. The scattering angle can therefore be used as a powerful bridge between scattering results and bound-state observables, allowing one to fully exploit the fact that it can be computed directly through both perturbative and numerical methods.

Regarding the PN determination of the linear-in-spin contributions to the conservative scattering angle, Ref. [94], which adapted the general strategy of Refs. [88–91] to spinning systems, extended the 4.5PN-accurate linear-in-spin result of Ref. [93] through the computation of the local 5.5PN terms [see Eq. (3.31) therein]. The resulting expression is determined up to a single undetermined coefficient in the ν^2 sector, $\mathsf{X}^{\nu^2}_{59}$, whose value awaits input from complementary higher-order approaches, such as second-order GSF calculations.

In the absence of a fully determined result, our aim here is to use the available scattering-angle components to derive, in gauge-general form, the corresponding 5.5PN local contributions to g_S and g_{S_*}.

To this end, we must compute the conservative scattering angle associated with our effective Hamiltonian. In general, the relation between the two is given by

$$\chi_{\rm eff} \equiv -\pi - 2\int_0^{u_{\rm max}} \frac{du}{u^2}\frac{\partial}{\partial p_\varphi} p_r(\hat{E}_{\rm eff}, p_\varphi, u), \tag{25}$$

where $p_r(\hat{E}_{\rm eff}, p_\varphi, u)$ is obtained from the iterative solution to the Hamilton-Jacobi equation in the effective problem, $u_{\rm max}$ denotes the largest root of $p_r(\hat{E}_{\rm eff}, p_\varphi, u) = 0$, and $\hat{E}_{\rm eff}$ is the rescaled effective energy, related to the effective Hamiltonian through the energy-conservation condition $\hat{H}_{\rm eff} = \hat{E}_{\rm eff}$. The subscript "eff" on the scattering angle is included to emphasize that the quantity is computed from $\hat{H}_{\rm eff}$.

To compute the local contribution to the scattering angle, the integral (25) must be evaluated using only the local part of the effective Hamiltonian, both in the EOB potentials and in the gyro-gravitomagnetic functions. As for the local 5.5PN contributions to the latter, and following the same strategy adopted in the previous section for the nonlocal terms, we introduce the most general ansatz compatible with this PN order, namely

$$\begin{aligned} g_S^{\rm 5.5PN,loc} = \frac{1}{c^8}\big(&g_1^{\rm N^4LO} p^8 + g_2^{\rm N^4LO} p^6 p_r^2 + g_3^{\rm N^4LO} p^4 p_r^4 \\ &+ g_4^{\rm N^4LO} p^2 p_r^6 + g_5^{\rm N^4LO} p_r^8 + g_6^{\rm N^4LO} p^6 u \\ &+ g_7^{\rm N^4LO} p^4 p_r^2 u + g_8^{\rm N^4LO} p^2 p_r^4 u + g_9^{\rm N^4LO} p_r^6 u \\ &+ g_{10}^{\rm N^4LO} p^4 u^2 + g_{11}^{\rm N^4LO} p^2 p_r^2 u^2 + g_{12}^{\rm N^4LO} p_r^4 u^2 \\ &+ g_{13}^{\rm N^4LO} p^2 u^3 + g_{14}^{\rm N^4LO} p_r^2 u^3 + g_{15}^{\rm N^4LO} u^4\big), \end{aligned} \tag{26}$$

where we have introduced a set of 15 coefficients, $g_n^{\rm N^4LO}$. An analogous ansatz, involving another set of 15 coefficients $g_{*n}^{\rm N^4LO}$, is used for $g_{S_*}^{\rm 5.5PN,loc}$. The different structure of this ansatz, as compared to Eq. (21), reflects the fact that in the local sector we neither perform a small-eccentricity expansion nor need to account for logarithmic contributions.

At this stage, the 5.5PN determination of $\chi_{\rm eff}$ is obtained by following the same procedure outlined in Sec. III B of Ref. [95], extending the simultaneous expansion of Eq. (25) in powers of $1/p_\varphi$ and $1/c$ up to orders $1/p_\varphi^5$ and $1/c^{10}$, respectively.

The resulting 5.5PN spin-orbit contribution to the scattering angle reads

$$\begin{aligned} \chi_{\rm eff}^{\rm 5.5\ PN,SO} = &S\chi_S^{\rm 5.5PN}(\hat{E}_{\rm eff}, p_\varphi, g_n^{\rm N^4LO}) \\ &+ S_*\chi_{S_*}^{\rm 5.5PN}(\hat{E}_{\rm eff}, p_\varphi, g_{*n}^{\rm N^4LO}), \end{aligned} \tag{27}$$

which exhibits two distinct linear-in-spin contributions, each depending on the coefficients of the general ansatz (26) and its $g_{S_*}^{\rm 5.5\ PN,loc}$ analog. The explicit expressions for both components are provided in the Supplemental Materials [97].

B. Local gyro-gravitomagnetic functions in full gauge generality at 5.5PN

We can now proceed to constrain the coefficients of our general ansatz by imposing the matching condition

$$\chi_{\rm eff}^{\rm 5.5\ PN,SO} = \chi_{\rm Khalil}^{\rm 5.5\ PN,SO}, \tag{28}$$

which follows from the gauge invariance of the scattering angle. Here $\chi_{\rm Khalil}^{\rm 5.5\ PN,SO}$ denotes the local linear-in-spin 5.5PN contribution to the scattering angle, given in Eq. (3.31) of Ref. [94].

From the S and S_* components of Eq. (28), we obtain two sets of five equations relating the coefficients of the local ansatz. An explicit example of a solution to these systems is provided in the Supplemental Materials [97].

Substituting such a solution into our general ansatz for $g_S^{5.5\ \mathrm{PN,loc}}$ and $g_{S_*}^{5.5\ \mathrm{PN,loc}}$, we finally obtain

$$
\begin{aligned}
g_S^{5.5\mathrm{PN,loc}} &= g_1^{\mathrm{N^4LO}} p^8 + \left(-\frac{27\nu}{64} + \frac{99\nu^2}{128} + \frac{945\nu^3}{256} + \frac{189\nu^4}{32} - 9g_1^{\mathrm{N^4LO}} - 3g_2^{\mathrm{N^4LO}} - \frac{9}{5}g_3^{\mathrm{N^4LO}} - \frac{9}{7}g_4^{\mathrm{N^4LO}}\right) p_r^8 \\
&+ (g_2^{\mathrm{N^4LO}} p_r^2 + g_6^{\mathrm{N^4LO}} u) p^6 + \left(\frac{16}{3}g_2^{\mathrm{N^3LO}} + 6g_4^{\mathrm{N^3LO}} + \frac{41}{7}g_7^{\mathrm{N^3LO}} - \frac{467\nu}{64} - \frac{1077\nu^2}{128} - \frac{3607\nu^3}{256} + \frac{1577\nu^4}{160}\right. \\
&\left. - 65g_1^{\mathrm{N^4LO}} - 11g_2^{\mathrm{N^4LO}} - \frac{17}{5}g_3^{\mathrm{N^4LO}} - g_4^{\mathrm{N^4LO}} - \frac{64}{5}g_6^{\mathrm{N^4LO}} - \frac{16}{5}g_7^{\mathrm{N^4LO}} - \frac{8}{5}g_8^{\mathrm{N^4LO}}\right) p_r^6 u + (g_3^{\mathrm{N^4LO}} p_r^4 \\
&+ g_7^{\mathrm{N^4LO}} p_r^2 u + g_{10}^{\mathrm{N^4LO}} u^2) p^4 + \left[6g_2^{\mathrm{N^2LO}} + \frac{64}{3}g_2^{\mathrm{N^3LO}} + \frac{79}{20}g_4^{\mathrm{N^2LO}} + \frac{88}{5}g_4^{\mathrm{N^3LO}} + \frac{3}{2}g_5^{\mathrm{N^3LO}} + \frac{377}{28}g_7^{\mathrm{N^3LO}}\right. \\
&+ \frac{7}{4}g_8^{\mathrm{N^3LO}} + \left(\frac{205}{4} + 6g_2^{\mathrm{N^2LO}} + 8g_2^{\mathrm{NLO}} + \frac{12}{5}g_4^{\mathrm{N^2LO}}\right)\nu + \left(\frac{30\,541}{128} - 6g_2^{\mathrm{NLO}}\right)\nu^2 - \frac{60\,813\nu^3}{256} - \frac{107\nu^4}{32} \\
&\left. - 95g_1^{\mathrm{N^4LO}} - 8g_2^{\mathrm{N^4LO}} - g_3^{\mathrm{N^4LO}} - 41g_6^{\mathrm{N^4LO}} - 5g_7^{\mathrm{N^4LO}} - g_8^{\mathrm{N^4LO}} - \frac{35}{3}g_{10}^{\mathrm{N^4LO}} - \frac{7}{3}g_{11}^{\mathrm{N^4LO}}\right] p_r^4 u^2 + \left[\frac{91}{6}g_2^{\mathrm{N^2LO}}\right. \\
&+ \frac{44}{5}g_2^{\mathrm{N^3LO}} + \frac{461}{60}g_2^{\mathrm{NLO}} + \frac{323}{50}g_4^{\mathrm{N^2LO}} + \frac{9}{5}g_4^{\mathrm{N^3LO}} + \frac{53}{20}g_5^{\mathrm{N^2LO}} + \frac{59}{10}g_5^{\mathrm{N^3LO}} - \frac{51}{28}g_7^{\mathrm{N^3LO}} + \frac{87}{20}g_8^{\mathrm{N^3LO}} \\
&+ \frac{1}{5}g_9^{\mathrm{N^3LO}} + \left(\frac{1\,869\,859}{1\,600} - 4g_2^{\mathrm{N^2LO}} + \frac{28}{5}g_2^{\mathrm{NLO}} - 6g_4^{\mathrm{N^2LO}} + 3g_5^{\mathrm{N^2LO}} - \frac{22\,301\pi^2}{256}\right)\nu + \left(\frac{877\,631}{960}\right. \\
&\left. - g_2^{\mathrm{NLO}} - \frac{1\,087\pi^2}{64}\right)\nu^2 - \frac{12\,579\nu^3}{128} + \frac{3\nu^4}{4} - 30g_1^{\mathrm{N^4LO}} - g_2^{\mathrm{N^4LO}} - 21g_6^{\mathrm{N^4LO}} - g_7^{\mathrm{N^4LO}} - 13g_{10}^{\mathrm{N^4LO}} - g_{11}^{\mathrm{N^4LO}} \\
&\left. - 6g_{13}^{\mathrm{N^4LO}}\right] p_r^2 u^3 + \left[\frac{1}{2}g_2^{\mathrm{N^2LO}} + \frac{2}{5}g_2^{\mathrm{N^3LO}} + \frac{101}{20}g_2^{\mathrm{NLO}} - \frac{369}{200}g_4^{\mathrm{N^2LO}} + \frac{39}{20}g_5^{\mathrm{N^2LO}} + \frac{9}{20}g_5^{\mathrm{N^3LO}} + \frac{3}{56}g_7^{\mathrm{N^3LO}}\right. \\
&- \frac{3}{40}g_8^{\mathrm{N^3LO}} + \frac{3}{5}g_9^{\mathrm{N^3LO}} + \left(-\frac{4\,546\,811}{14\,400} - \frac{1}{2}g_2^{\mathrm{N^2LO}} - \frac{4\,681}{180}g_2^{\mathrm{NLO}} + \frac{3}{20}g_4^{\mathrm{N^2LO}} - \frac{3}{4}g_5^{\mathrm{N^2LO}} + \frac{62\,041\pi^2}{1\,536}\right. \\
&\left. + \frac{41\pi^2 g_2^{\mathrm{NLO}}}{48}\right)\nu + \left(\frac{313\,823}{5\,760} - \frac{1\,225\pi^2}{384} - \frac{3\mathsf{X}_{59}^{\nu^2}}{16}\right)\nu^2 - \frac{239\nu^3}{256} - \frac{\nu^4}{32} - g_1^{\mathrm{N^4LO}} - g_6^{\mathrm{N^4LO}} - g_{10}^{\mathrm{N^4LO}} \\
&\left. - g_{13}^{\mathrm{N^4LO}}\right] u^4 + (g_4^{\mathrm{N^4LO}} p_r^6 + g_8^{\mathrm{N^4LO}} p_r^4 u + g_{11}^{\mathrm{N^4LO}} p_r^2 u^2 + g_{13}^{\mathrm{N^4LO}} u^3) p^2, \qquad (29a)
\end{aligned}
$$

$$
\begin{aligned}
g_{S_*}^{5.5\mathrm{PN,loc}} &= g_{*1}^{\mathrm{N^4LO}} p^8 + \left(\frac{693}{256} + \frac{189}{64}\nu + \frac{1\,053}{256}\nu^2 + \frac{315}{64}\nu^3 + \frac{945}{256}\nu^4 - 9g_{*1}^{\mathrm{N^4LO}} - 3g_{*2}^{\mathrm{N^4LO}} - \frac{9}{5}g_{*3}^{\mathrm{N^4LO}}\right. \\
&\left. - \frac{9}{7}g_{*4}^{\mathrm{N^4LO}}\right) p_r^8 + (g_{*2}^{\mathrm{N^4LO}} p_r^2 + g_{*6}^{\mathrm{N^4LO}} u) p^6 + \left(\frac{7\,245}{256} + \frac{16}{3}g_{*2}^{\mathrm{N3LO}} + 6g_{*4}^{\mathrm{N3LO}} + \frac{41}{7}g_{*7}^{\mathrm{N3LO}} + \frac{1\,333}{64}\nu\right. \\
&+ \frac{4\,533}{256}\nu^2 + \frac{3\,759}{320}\nu^3 + \frac{16\,077}{1\,280}\nu^4 - 65g_{*1}^{\mathrm{N^4LO}} - 11g_{*2}^{\mathrm{N^4LO}} - \frac{17}{5}g_{*3}^{\mathrm{N^4LO}} - g_{*4}^{\mathrm{N^4LO}} - \frac{64}{5}g_{*6}^{\mathrm{N^4LO}} - \frac{16}{5}g_{*7}^{\mathrm{N^4LO}} \\
&\left. - \frac{8}{5}g_{*8}^{\mathrm{N^4LO}}\right) p_r^6 u + (g_{*3}^{\mathrm{N^4LO}} p_r^4 + g_{*7}^{\mathrm{N^4LO}} p_r^2 u + g_{*10}^{\mathrm{N^4LO}} u^2) p^4 + \left[\frac{12\,663}{256} + 6g_{*2}^{\mathrm{N2LO}} + \frac{64}{3}g_{*2}^{\mathrm{N3LO}} + \frac{79}{20}g_{*4}^{\mathrm{N2LO}}\right. \\
&+ \frac{88}{5}g_{*4}^{\mathrm{N3LO}} + \frac{3}{2}g_{*5}^{\mathrm{N3LO}} + \frac{377}{28}g_{*7}^{\mathrm{N3LO}} + \frac{7}{4}g_{*8}^{\mathrm{N3LO}} + \left(\frac{3\,297}{64} + 6g_{*2}^{\mathrm{N2LO}} + 8g_{*2}^{\mathrm{NLO}} + \frac{12}{5}g_{*4}^{\mathrm{N2LO}}\right)\nu + \left(\frac{19\,467}{256}\right. \\
&\left. - 6g_{*2}^{\mathrm{NLO}}\right)\nu^2 - \frac{11\,523}{64}\nu^3 - \frac{1\,377}{256}\nu^4 - 95g_{*1}^{\mathrm{N^4LO}} - 8g_{*2}^{\mathrm{N^4LO}} - g_{*3}^{\mathrm{N^4LO}} - 41g_{*6}^{\mathrm{N^4LO}} - 5g_{*7}^{\mathrm{N^4LO}} - g_{*8}^{\mathrm{N^4LO}} \\
&\left. - \frac{35}{3}g_{*10}^{\mathrm{N^4LO}} - \frac{7}{3}g_{*11}^{\mathrm{N^4LO}}\right] p_r^4 u^2 + \left[\frac{13\,577}{640} + \frac{91}{6}g_{*2}^{\mathrm{N2LO}} + \frac{44}{5}g_{*2}^{\mathrm{N3LO}} + \frac{461}{60}g_{*2}^{\mathrm{NLO}} + \frac{323}{50}g_{*4}^{\mathrm{N2LO}} + \frac{9}{5}g_{*4}^{\mathrm{N3LO}}\right.
\end{aligned}
$$

$$+\frac{53}{20}g_{*5}^{\mathrm{N2LO}}+\frac{59}{10}g_{*5}^{\mathrm{N3LO}}-\frac{51}{28}g_{*7}^{\mathrm{N3LO}}+\frac{87}{20}g_{*8}^{\mathrm{N3LO}}+\frac{1}{5}g_{*9}^{\mathrm{N3LO}}+\left(\frac{27\,739}{80}-4g_{*2}^{\mathrm{N2LO}}+\frac{28}{5}g_{*2}^{\mathrm{NLO}}-6g_{*4}^{\mathrm{N2LO}}\right.$$
$$\left.+3g_{*5}^{\mathrm{N2LO}}-\frac{4\,829\pi^2}{256}\right)\nu+\left(\frac{360\,199}{640}-g_{*2}^{\mathrm{NLO}}-\frac{123\pi^2}{8}\right)\nu^2-\frac{2\,931}{32}\nu^3+\frac{171}{128}\nu^4-30g_{*1}^{\mathrm{N4LO}}-g_{*2}^{\mathrm{N4LO}}$$
$$-21g_{*6}^{\mathrm{N4LO}}-g_{*7}^{\mathrm{N4LO}}-13g_{*10}^{\mathrm{N4LO}}-g_{*11}^{\mathrm{N4LO}}-6g_{*13}^{\mathrm{N4LO}}\Big]p_r^2u^3+\Big[-\frac{2\,103}{1\,280}+\frac{1}{2}g_{*2}^{\mathrm{N2LO}}+\frac{2}{5}g_{*2}^{\mathrm{N3LO}}+\frac{101}{20}g_{*2}^{\mathrm{NLO}}$$
$$-\frac{369}{200}g_{*4}^{\mathrm{N2LO}}+\frac{39}{20}g_{*5}^{\mathrm{N2LO}}+\frac{9}{20}g_{*5}^{\mathrm{N3LO}}+\frac{3}{56}g_{*7}^{\mathrm{N3LO}}-\frac{3}{40}g_{*8}^{\mathrm{N3LO}}+\frac{3}{5}g_{*9}^{\mathrm{N3LO}}+\left(-\frac{9\,785}{192}-\frac{1}{2}g_{*2}^{\mathrm{N2LO}}\right.$$
$$\left.-\frac{4\,681}{180}g_{*2}^{\mathrm{NLO}}+\frac{3}{20}g_{*4}^{\mathrm{N2LO}}-\frac{3}{4}g_{*5}^{\mathrm{N2LO}}+\frac{26\,943\pi^2}{2\,048}+\frac{41}{48}g_{*2}^{\mathrm{NLO}}\pi^2\right)\nu+\left(\frac{9\,729}{1\,280}-\frac{123\pi^2}{64}-\frac{3}{16}\mathsf{X}_{59}^{\nu^2}\right)\nu^2$$
$$-\frac{57}{64}\nu^3-\frac{15}{256}\nu^4-g_{*1}^{\mathrm{N4LO}}-g_{*6}^{\mathrm{N4LO}}-g_{*10}^{\mathrm{N4LO}}-g_{*13}^{\mathrm{N4LO}}\Big]u^4+(g_{*4}^{\mathrm{N4LO}}p_r^6+g_{*8}^{\mathrm{N4LO}}p_r^4u$$
$$+g_{*11}^{\mathrm{N4LO}}p_r^2u^2+g_{*13}^{\mathrm{N4LO}}u^3)p^2. \tag{29b}$$

The remaining ten coefficients in each of these expressions encode the freedom associated with the spin-gauge choice, in direct analogy with the coefficients appearing in Eqs. (24).

In accordance with the local/nonlocal decomposition of Eq. (3), the full gauge-general expressions for $g_S^{5.5\mathrm{PN}}$ and $g_{S_*}^{5.5\mathrm{PN}}$ are obtained by combining Eqs. (24) and (29). Since these results constitute one of the main outcomes of this work, we provide their complete expressions in electronic form in the Supplemental Materials [97].

V. ANALYTICAL CONSISTENCY CHECKS: GAUGE INVARIANT QUANTITIES

In this section, we test the validity of our gauge-general results for the 5.5PN gyro-gravitomagnetic functions. To this end, we compute the 5.5PN linear-in-spin contributions to two gauge-invariant quantities: the binding energy and the fractional periastron advance for quasicircular orbits. A necessary consistency requirement for the gauge-general expressions of $g_S^{5.5\mathrm{PN}}$ and $g_{S_*}^{5.5\mathrm{PN}}$ is that any gauge-invariant observable must remain independent of the 30 gauge coefficients (10 local and 20 nonlocal) entering these functions.

The rescaled effective binding energy has been computed up to 4.5PN order in Refs. [93,95] and up to 5.5PN order in Ref. [94]. It is defined as

$$E_b\equiv\hat{H}_{\mathrm{EOB}}^{\mathrm{circ}}(x)-\frac{1}{\nu}, \tag{30}$$

where the rescaled EOB Hamiltonian (16), evaluated along circular orbits, is expressed in terms of the frequency parameter $x\equiv\Omega_\varphi^{2/3}$, with Ω_φ the orbital frequency. Further details on the computation of $\hat{H}_{\mathrm{EOB}}^{\mathrm{circ}}(x)$ from the general-orbit EOB Hamiltonian can be found in Sec. IV of Ref. [95].

Turning to the fractional periastron advance per radial period, its definition is

$$K=1+\frac{\Delta\Phi}{2\pi}, \tag{31}$$

and, more explicitly, for quasicircular orbits one has

$$K\equiv\frac{\Omega_\varphi}{\Omega_r}\Big|_{\mathrm{circ}}=\left(\frac{\partial^2\hat{H}_{\mathrm{eff}}}{\partial r^2}\frac{\partial^2\hat{H}_{\mathrm{eff}}}{\partial p_r^2}\right)^{-1}\frac{\partial\hat{H}_{\mathrm{eff}}}{\partial p_\varphi}\Big|_{\mathrm{circ}}, \tag{32}$$

where the circular limit is taken only after the derivatives have been evaluated by subsequently rewriting all quantities in terms of the frequency parameter x. K has been computed to 3.5PN order in Ref. [109] and to 4.5PN order in Ref. [95].

Computing the linear-in-spin 5.5PN contributions to E_b and K using our gauge-general expressions for g_S and g_{S_*} in the Hamiltonian, we find

$$E_b^{5.5\ \mathrm{PN,SO}}=x^{13/2}\Big\{S\Big[-\frac{4\,725}{32}+\left(-\frac{1\,975\,415}{5184}+\frac{2\,425}{864}\pi^2+\frac{5}{8}\mathsf{X}_{59}^{\nu^2}\right)\nu^2+\frac{310\,795}{5184}\nu^3+\frac{35}{1458}\nu^4$$
$$+\nu\left(\frac{1\,411\,663}{640}+\frac{352}{3}\gamma_E-\frac{10\,325}{64}\pi^2+\frac{2\,080}{9}\log 2+\frac{176}{3}\log x\right)\Big]$$
$$+S_*\Big[-\frac{2\,835}{128}+\left(-\frac{275\,245}{3\,456}-\frac{205}{576}\pi^2+\frac{5}{8}\mathsf{X}_{59}^{\nu^2}\right)\nu^2+\frac{46\,765}{864}\nu^3+\frac{875}{31\,104}\nu^4$$
$$+\nu\left(\frac{126\,715}{144}+\frac{160}{3}\gamma_E-\frac{102\,355}{1\,536}\pi^2+\frac{992}{9}\log 2+\frac{80}{3}\log x\right)\Big]\Big\}, \tag{33}$$

$$K^{5.5\,\mathrm{PN,SO}} = x^{11/2}\Bigg\{S\Bigg[-\frac{23\,625}{2}+\left(-\frac{4\,266\,299}{288}+\frac{47\,263}{192}\pi^2+\frac{15}{4}\mathsf{X}_{59}^{\nu^2}\right)\nu^2+\frac{251\,375}{324}\nu^3-\frac{32}{81}\nu^4 + \nu\left(\frac{3\,259\,681\,769}{86\,400}+\frac{112\,528}{45}\gamma_E-\frac{1\,345\,253}{1\,152}\pi^2+\frac{48\,784}{45}\log 2+\frac{25\,272}{5}\log 3 - 1280\log 2+\frac{56\,264}{45}\log x\right)\Bigg] + S_*\Bigg[-\frac{42\,525}{8}+\left(-\frac{326\,597}{32}+\frac{11\,931}{64}\pi^2+\frac{15}{4}\mathsf{X}_{59}^{\nu^2}\right)\nu^2 + \frac{2\,737}{4}\nu^3-\frac{11}{27}\nu^4+\nu\left(\frac{114\,877\,897}{5\,760}+\frac{24\,208}{15}\gamma_E-\frac{1\,679\,935}{3\,072}\pi^2+\frac{8\,656}{15}\log 2+\frac{17\,496}{5}\log 3 - 960\log 2+\frac{12\,104}{15}\log x\right)\Bigg]\Bigg\}. \tag{34}$$

As expected, neither of the two expressions exhibits any residual dependence on the gauge coefficients. The only remaining parameter, $\mathsf{X}_{59}^{\nu^2}$, reflects the current incompleteness in the knowledge of the local linear-in-spin contribution to the 5.5PN scattering angle, as discussed in Sec. IV.

We further observe that the binding energy (33) is in perfect agreement with the 5.5PN result of Ref. [94].

VI. GAUGE FLEXIBILITY OF THE GYRO-GRAVITOMAGNETIC FUNCTIONS

In this section, building on our gauge-general results for $g_S^{5.5\mathrm{PN}}$ and $g_{S_*}^{5.5\mathrm{PN}}$, we investigate how different spin gauge choices at this order compare with numerical data. In particular, following Ref. [95], we focus on the DJS and $\overline{\mathrm{DJS}}$ spin gauges and examine their performance in reproducing the spin-orbit contribution to the circular-orbit binding energy.

A. The DJS spin gauge

The DJS spin gauge was first introduced in Ref. [82] and subsequently adopted in a wide range of works [84,93,95,110]. Its defining condition is straightforward: the gauge coefficients entering g_S and g_{S_*} must be fixed so as to eliminate any dependence on the total momentum p^2, or equivalently on the angular momentum p_φ. Imposing this gauge-fixing condition on our combined expressions (24a)+(29a) and (24b)+(29b) yields a system of equations that can be uniquely solved for all gauge coefficients. The corresponding solution, provided in the Supplemental Materials [97], gives the following 5.5PN expressions of the DJS gyro-gravitomagnetic functions:

$$(g_S^{5.5\mathrm{PN}})_{\mathrm{DJS}} = \left[\frac{31\,913}{128}\nu^2-\frac{73\,547}{256}\nu^3-\frac{107}{32}\nu^4+\nu\left(\frac{3\,325\,823}{1920}-\frac{1\,270\,912\ \log 2}{9}+\frac{437\,886\ \log 3}{5}\right)\right]p_r^4u^2 + \left[-\frac{2\,553}{128}\nu^2-\frac{11\,397}{256}\nu^3+\frac{1\,577}{160}\nu^4+\nu\left(\frac{9\,768\,651}{3200}+\frac{353\,598\,464\ \log 2}{225}-\frac{2\,517\,237\ \log 3}{5} - \frac{3\,015\,625\ \log 5}{9}\right)\right]p_r^6u + \left[\frac{99}{128}\nu^2+\frac{945}{256}\nu^3+\frac{189}{32}\nu^4+\nu\left(\frac{32\,193\,611}{11200}-\frac{1\,797\,965\,696\ \log 2}{189} - \frac{31\,129\,029\ \log 3}{200}+\frac{6\,352\,671\,875\ \log 5}{1512}\right)\right]p_r^8 + \left[\left(\frac{198\,133}{192}-\frac{1087\pi^2}{64}\right)\nu^2-\frac{8\,259}{64}\nu^3+\frac{3}{4}\nu^4 + \nu\left(\frac{27\,198\,169}{9600}-208\gamma_E-\frac{22\,301\pi^2}{256}+\frac{65\,488\ \log 2}{15}-\frac{23\,328\ \log 3}{5}\right)-104\nu\log u\right]p_r^2u^3 + \left[\left(\frac{235\,111}{1152}-\frac{583\pi^2}{96}-\frac{3}{16}\mathsf{X}_{59}^{\nu^2}\right)\nu^2-\frac{413}{256}\nu^3-\frac{1}{32}\nu^4+\nu\left(-\frac{12\,015\,517}{28\,800}-\frac{1\,168}{15}\gamma_E + \frac{620\,41\pi^2}{1536}-\frac{464\ \log 2}{3}\right)-\frac{584}{15}\nu\log u\right]u^4, \tag{35a}$$

$$
\begin{aligned}
(g_{S_*}^{5.5\mathrm{PN}})_{\mathrm{DJS}} = &\left[\frac{2\,525}{256}+\frac{12\,135}{256}\nu^2-\frac{13\,905}{64}\nu^3-\frac{1\,377}{256}\nu^4+\nu\left(\frac{37\,463}{40}-\frac{1\,489\,312\ \log 2}{15}+\frac{309\,096\ \log 3}{5}\right)\right]p_r^4u^2\\
&+\left[\frac{3\,555}{256}-\frac{879}{256}\nu^2-\frac{2\,391}{320}\nu^3+\frac{16\,077}{1\,280}\nu^4+\nu\left(\frac{795\,077}{400}+\frac{748\,718\,336\ \log 2}{675}-\frac{1\,799\,901\ \log 3}{5}\right.\right.\\
&\left.\left.-\frac{6\,296\,875\ \log 5}{27}\right)\right]p_r^6u+\left[\frac{693}{256}+\frac{1\,053}{256}\nu^2+\frac{315}{64}\nu^3+\frac{945}{256}\nu^4+\nu\left(\frac{20\,870\,707}{11\,200}-\frac{4\,538\,197\,984\ \log 2}{675}\right.\right.\\
&\left.\left.-\frac{2\,092\,959\ \log 3}{28}+\frac{2\,226\,734\,375\ \log 5}{756}\right)\right]p_r^8+\left[-\frac{27}{32}+\left(\frac{77\,201}{128}-\frac{123\pi^2}{8}\right)\nu^2-\frac{489}{4}\nu^3+\frac{171}{128}\nu^4\right.\\
&+\nu\left(\frac{1\,432\,861}{960}-\frac{512}{5}\gamma_E-\frac{4\,829\pi^2}{256}+\frac{46\,976\ \log 2}{15}-\frac{16\,038\ \log 3}{5}\right)-\frac{256}{5}\nu\ \log\ u\Big]p_r^2u^3\\
&+\left[-\frac{1\,701}{256}+\left(\frac{29\,081}{256}-\frac{123\pi^2}{32}-\frac{3}{16}\mathsf{X}_{59}^{\nu^2}\right)\nu^2-\frac{111}{64}\nu^3-\frac{15}{256}\nu^4+\nu\left(-\frac{1\,017}{20}-48\gamma_E\right.\right.\\
&\left.\left.+\frac{23\,663\pi^2}{2048}-\frac{1\,456\ \log 2}{15}\right)-24\nu\ \log\ u\right]u^4. \qquad (35b)
\end{aligned}
$$

We observe that these expressions are in exact agreement with Eqs. (2.24), (3.32), and (3.33) of Ref. [94], where the computation was carried out entirely within the DJS spin gauge, i.e., by imposing this gauge choice directly at the level of the ansatz for the two gyro-gravitomagnetic functions.

B. The $\overline{\mathrm{DJS}}$ spin gauge

We now turn to a notable alternative to the DJS spin gauge, introduced in Ref. [111] and further explored in Ref. [95], namely the $\overline{\mathrm{DJS}}$ spin gauge.

The defining feature of this spin gauge is the requirement that, at each available PN order, the condition

$$
g_{S_*}^{\overline{\mathrm{DJS}}} \longrightarrow [\nu \to 0] g_{S_*}^{\mathrm{K}}, \qquad (36)
$$

be satisfied; that is, in the test-mass limit, g_{S_*} must reduce to the gyro-gravitomagnetic function of a spinning test particle in a Kerr background, denoted by $g_{S_*}^{\mathrm{K}}$. The full expression of the latter is [112][3]

$$
g_{S_*}^{K} = \frac{1}{u}\left\{\sqrt{\frac{A^K}{W^K}}\left[1-\sqrt{\frac{A^K}{D^K}}\right]-\frac{u\partial_u A^K}{2(1+\sqrt{W^K})\sqrt{D^K}}\right\}, \qquad (37)
$$

where A^K and D^K are the EOB potentials in the limit $\nu \to 0$ (with $D = \bar{D}^{-1}$) and

$$
W^K \equiv 1 + p_\varphi^2 u^2 + \frac{A^K}{D^K} p_r^2. \qquad (38)
$$

This gauge-fixing choice is motivated by the fact that, in the test-mass limit $\nu \to 0$, the function g_S^{DJS} trivially reduces to its Kerr value $g_S^{\mathrm{K}} = 2$, whereas $g_{S_*}^{\mathrm{DJS}}$ reproduces only the PN expansion of $g_{S_*}^{\mathrm{K}}$ in the circular limit. In contrast, in the $\overline{\mathrm{DJS}}$ spin gauge the test-mass limit is, by construction, enforced to reduce *both* gyro-gravitomagnetic functions to their exact Kerr expressions for a spinning test particle.

It is important to stress that this gauge condition alone is not sufficient to fully fix the spin gauge. Since it constrains only the test-mass limit of the gyro-gravitomagnetic functions, it determines solely the $\mathcal{O}(\nu^0)$ part of the spin-gauge coefficients. To completely fix the gauge, we therefore supplement the test-mass condition with the additional requirement that all remaining ν-dependent components of the gauge coefficients vanish.[4]

By imposing these conditions, we obtain a second system of equations that can be solved to fully determine all gauge coefficients; the corresponding solution is also

[3]Since we neglect spin contributions beyond linear order, we do not include in $g_{S_*}^{\mathrm{K}}$ any dependence on the effective centrifugal radius r_c.

[4]We also explored an alternative supplementary condition beyond the test-mass limit, namely the suppression of any dependence on $\dot{p}_r$. Since the resulting gyro-gravitomagnetic functions are numerically nearly indistinguishable from those obtained with our chosen condition, we adopt the latter for its greater simplicity.

provided in the Supplemental Materials [97]. The resulting 5.5PN gyro-gravitomagnetic functions in the $\overline{\text{DJS}}$ gauge are

$$
\begin{aligned}
(g_{S_*}^{5.5\text{PN}})_{\overline{\text{DJS}}} = {}& \left(\frac{77}{256}+\frac{189}{64}\nu+\frac{1053}{256}\nu^2+\frac{315}{64}\nu^3+\frac{945}{256}\nu^4\right)p_r^8+\left(\frac{145}{64}+\frac{1333}{64}\nu+\frac{4533}{256}\nu^2+\frac{3759}{320}\nu^3\right.\\
&\left.+\frac{16077}{1280}\nu^4\right)p_r^6u+\left[\frac{77}{64}p_\varphi^2p_r^6+\left(\frac{37}{16}+\frac{3297}{64}\nu+\frac{19467}{256}\nu^2-\frac{11523}{64}\nu^3-\frac{1377}{256}\nu^4\right)p_r^4\right]u^2\\
&+\left[\frac{75}{16}p_\varphi^2p_r^4+\left[-\frac{3}{16}+\left(\frac{28039}{80}-\frac{4829}{256}\pi^2\right)\nu+\left(\frac{360199}{640}-\frac{123}{8}\pi^2\right)\nu^2-\frac{2931}{32}\nu^3+\frac{171}{128}\nu^4\right]p_r^2\right]u^3\\
&+\left[-\frac{7}{8}+\frac{3}{8}p_\varphi^2p_r^2+\frac{231}{128}p_\varphi^4p_r^4+\left(\frac{9729}{1280}-\frac{123}{64}\pi^2-\frac{3}{16}\mathsf{X}_{59}^{\nu^2}\right)\nu^2-\frac{57}{64}\nu^3-\frac{15}{256}\nu^4+\nu\left(-\frac{7277321473}{11200}\right.\right.\\
&\left.+\frac{1646928}{25}\gamma_E+\frac{26943}{2048}\pi^2-\frac{5021084624}{189}\log 2+\frac{1422585909}{140}\log 3+\frac{3788359375}{756}\log 5\right)\\
&\left.+\frac{823464}{25}\nu\log u\right]u^4+\left\{\frac{165}{64}p_\varphi^4p_r^2+p_\varphi^2\left[\frac{5}{16}+\nu\left(\frac{2796846856}{525}-\frac{13503488}{25}\gamma_E+\frac{1023479286464}{4725}\log 2\right.\right.\right.\\
&\left.\left.\left.-\frac{2916358668}{35}\log 3-\frac{7664875000}{189}\log 5\right)-\frac{6751744}{25}\nu\log u\right]\right\}u^5+\left\{\frac{77}{64}p_\varphi^6p_r^2+p_\varphi^4\left[-\frac{3}{16}\right.\right.\\
&\left.\left.+\nu\left(-\frac{57161452}{3}+1930752\gamma_E-\frac{520306868128}{675}\log 2+\frac{1490245128}{5}\log 3+\frac{3870218750}{27}\log 5\right)\right.\right.\\
&\left.\left.+965376\nu\log u\right]\right)u^6+\left[\nu\left(\frac{996988856}{25}-\frac{100917248}{25}\gamma_E+\frac{43060589504}{27}\log 2-\frac{3117148596}{5}\log 3\right.\right.\\
&\left.\left.-\frac{7891562500}{27}\log 5\right)-\frac{50458624}{25}\nu\log u\right]p_\varphi^{10}u^9+\left[\frac{5}{32}+\nu\left(\frac{582338384}{15}-3932160\gamma_E\right.\right.\\
&\left.\left.+\frac{1055323161856}{675}\log 2-\frac{3036137742}{5}\log 3-\frac{7803406250}{27}\log 5\right)-1966080\nu\log u\right]p_\varphi^6u^7\\
&+\left[\nu\left(\frac{40346688}{7}-\frac{2916352}{5}\gamma_E+\frac{1085740722176}{4725}\log 2-\frac{3152617362}{35}\log 3-\frac{7929343750}{189}\log 5\right)\right.\\
&\left.-\frac{1458176}{5}\nu\log u\right]p_\varphi^{14}u^{11}+\left[\nu\left(-\frac{1507161628}{75}+\frac{50843648}{25}\gamma_E-\frac{541332696992}{675}\log 2+314079444\log 3\right.\right.\\
&\left.\left.+\frac{3958375000}{27}\log 5\right)+\frac{25421824}{25}\nu\log u\right]p_\varphi^{12}u^{10}+\left[\frac{77}{256}+\nu\left(-\frac{739106572}{15}+4988928\gamma_E\right.\right.\\
&\left.\left.-\frac{266838974336}{135}\log 2+\frac{1541014875}{2}\log 3+\frac{19634453125}{54}\log 5\right)+2494464\nu\log u\right]p_\varphi^8u^8, \qquad (39a)
\end{aligned}
$$

$$
\begin{aligned}
(g_S^{5.5\text{PN}})_{\overline{\text{DJS}}} = {}& p_r^4u^2\left(\frac{205}{4}\nu+\frac{30541}{128}\nu^2-\frac{60813}{256}\nu^3-\frac{107}{32}\nu^4\right)+p_r^2u^3\left[\left(\frac{1869859}{1600}-\frac{22301\pi^2}{256}\right)\nu\right.\\
&\left.+\left(\frac{877631}{960}-\frac{1087\pi^2}{64}\right)\nu^2-\frac{12579}{128}\nu^3+\frac{3}{4}\nu^4\right]+p_r^8\left(-\frac{27}{64}\nu+\frac{99}{128}\nu^2+\frac{945}{256}\nu^3+\frac{189}{32}\nu^4\right)\\
&+p_r^6u\left(-\frac{467}{64}\nu-\frac{1077}{128}\nu^2-\frac{3607}{256}\nu^3+\frac{1577}{160}\nu^4\right)+p_\varphi^{10}u^9\left[\nu\left(\frac{4144026748}{75}-\frac{40997632}{5}\gamma_E\right.\right.\\
&\left.\left.+\frac{304929978368\ \log 2}{135}-\frac{22040831187\ \log 3}{25}-\frac{11292265625\ \log 5}{27}\right)-\frac{20498816}{5}\nu\ \log\ u\right]\\
&+p_\varphi^6u^7\left[\nu\left(\frac{4033101256}{75}-7987200\gamma_E+\frac{1494627871744\ \log 2}{675}-\frac{21466187217\ \log 3}{25}\right.\right.\\
&\left.\left.-\frac{11165609375\ \log 5}{27}\right)-3993600\nu\ \log\ u\right]+p_\varphi^{14}u^{11}\left[\nu\left(\frac{4193060296}{525}-1184768\gamma_E\right.\right.
\end{aligned}
$$

$$+\frac{1\,537\,720\,290\,304\ \log 2}{4725}-\frac{22\,292\,460\,117\ \log 3}{175}-\frac{11\,346\,546\,875\ \log 5}{189}\Big)-592\,384\nu\ \log u\Big]$$
$$+p_\varphi^2u^5\Big[\nu\Big(\frac{258\,162\,588}{35}-\frac{5\,485\,792}{5}\gamma_E+\frac{1\,449\,515\,277\,856\ \log 2}{4725}-\frac{20\,616\,856\,047\ \log 3}{175}$$
$$-\frac{10\,966\,578\,125\ \log 5}{189}\Big)-\frac{2\,742\,896}{5}\nu\ \log u\Big]+u^4\Big[\Big(\frac{313\,823}{5\,760}-\frac{1\,225\pi^2}{384}-\frac{3}{16}\mathsf{X}_{59}^{\nu^2}\Big)\nu^2-\frac{239}{256}\nu^3$$
$$-\frac{1}{32}\nu^4+\nu\Big(-\frac{90\,682\,596\,509}{100\,800}+\frac{2\,007\,488}{15}\gamma_E+\frac{62\,041\pi^2}{1\,536}-\frac{35\,555\,719\,744\ \log 2}{945}+\frac{20\,112\,254\,397\ \log 3}{1\,400}$$
$$+\frac{10\,839\,921\,875\ \log 5}{1\,512}\Big)+\frac{1\,003\,744}{15}\nu\ \log u\Big]+p_\varphi^{16}u^{12}\Big[\nu\Big(-\frac{524\,132\,537}{525}+148\,096\gamma_E$$
$$-\frac{192\,215\,036\,288\ \log 2}{4\,725}+\frac{22\,292\,460\,117\ \log 3}{1\,400}+\frac{11\,346\,546\,875\ \log 5}{1\,512}\Big)+74\,048\nu\ \log u\Big]$$
$$+p_\varphi^4u^6\Big[\nu\Big(-\frac{659\,682\,546}{25}+3\,921\,840\gamma_E-\frac{736\,894\,566\,512\ \log 2}{675}+\frac{21\,071\,552\,787\ \log 3}{50}$$
$$+\frac{11\,075\,140\,625\ \log 5}{54}\Big)+1\,960\,920\nu\ \log u\Big]+p_\varphi^{12}u^{10}\Big[\nu\Big(-\frac{417\,671\,578}{15}+\frac{20\,655\,232}{5}\gamma_E$$
$$-\frac{766\,681\,745\,408\ \log 2}{675}+\frac{22\,208\,583\,807\ \log 3}{50}+\frac{11\,328\,453\,125\ \log 5}{54}\Big)+\frac{10\,327\,616}{5}\nu\log u\Big]$$
$$+p_\varphi^8u^8\Big[\nu\Big(-\frac{1\,023\,922\,606}{15}+10\,133\,760\gamma_E-\frac{75\,583\,730\,432\ \log 2}{27}+\frac{21\,791\,700\,297\ \log 3}{20}$$
$$+\frac{56\,189\,921\,875\ \log 5}{108}\Big)+5\,066\,880\nu\ \log u\Big]. \tag{39b}$$

In this case, we have used the three dynamical variables (u, p_r, p_φ) instead of (u, p_r, p^2), as this choice simplifies the structure of our results. The corresponding expressions in terms of (u, p_r, p^2) can be recovered straightforwardly by using the relation $p_\varphi = u\sqrt{p^2 - p_r^2}$.

C. Performance comparison: Binding energy in the DJS and $\overline{\text{DJS}}$ spin gauges

In this subsection, we assess the performance of the two spin gauges introduced above. To this end, we numerically compute the spin-orbit contribution to the binding energy, $E_b^{\rm SO}$, for circular orbits in both the DJS and $\overline{\text{DJS}}$ gauges, and compare the resulting curves with those extracted from NR simulations. Although the circular-orbit binding energy is a gauge-invariant quantity and is, in principle, independent of the chosen spin gauge, this invariance holds strictly only up to the perturbative order to which the conservative dynamics is known. We therefore exploit the residual gauge dependence that arises when the binding energy is computed using truncated PN series, and use it as a diagnostic to compare the performance of the two spin gauges.[5]

To compute the analytical binding–energy curves from the EOB Hamiltonian, we begin by imposing the two circular-limit conditions

$$\left.\frac{d\hat{H}_{\rm EOB}(r, p_r, p_\varphi, \mathsf{X}_{59}^{\nu^2})}{dr}\right|_{p_r\to 0} = 0, \tag{40a}$$

$$\left.\left(\frac{d\hat{H}_{\rm EOB}(r, p_r, p_\varphi, \mathsf{X}_{59}^{\nu^2})}{dp_\varphi}\right)^{1/3}\right|_{p_r\to 0} = v_\omega, \tag{40b}$$

which are solved simultaneously for r and p_φ for any given value of $v_\omega \equiv \Omega_\varphi^{1/3}$. The resulting values of r and p_φ are then substituted directly into the circular-orbit binding energy[6]

$$E_b(r, p_\varphi) = \hat{H}_{\rm EOB}|_{p_r\to 0} - \frac{1}{\nu}, \tag{41}$$

from which the spin-orbit contribution is isolated via the relation [113]

[5]Similar comparison strategies have been employed in Refs. [94,95], and in particular in Ref. [92].

[6]We note that this differs from Eq. (30), where $\hat{H}_{\rm EOB}$, and thus E_b, is expressed in terms of x.

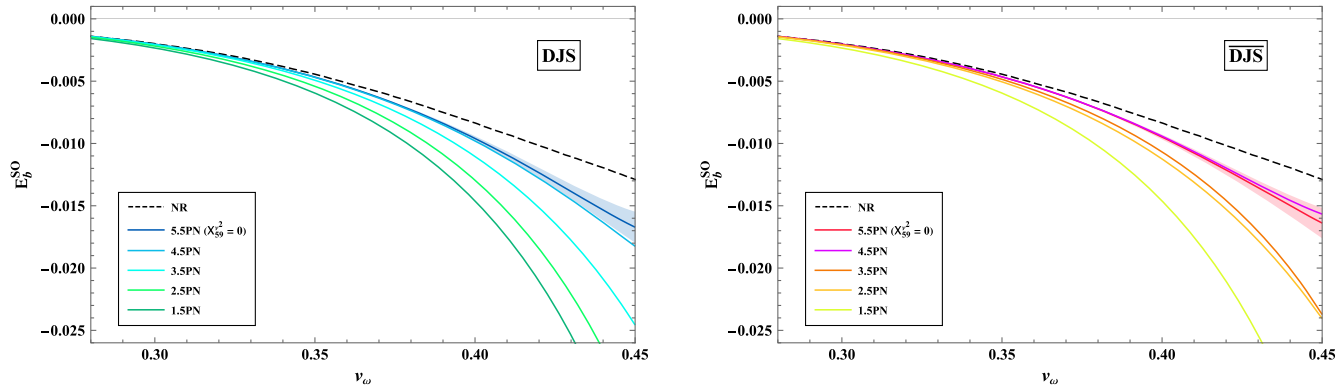

FIG. 1. Spin-orbit contribution to the binding energy for circular orbits as a function of v_ω, shown in the DJS (left panel) and $\overline{\text{DJS}}$ (right panel) spin gauges. In each panel, the numerical curve from Ref. [113] is displayed as a black dashed line, together with the analytical curves obtained by truncating the spin-orbit sector of the EOB Hamiltonian at different PN orders (see the legend in the insets). At 5.5PN order, the $X_{59}^{\nu^2}=0$ curve is accompanied by a shaded band indicating the variation induced by changing $X_{59}^{\nu^2}$ within the range $[-750, 750]$. The upper edge of the shaded region corresponds to $X_{59}^{\nu^2}=750$, while decreasing $X_{59}^{\nu^2}$ produces a systematic downward shift of the curves, with the lower edge reached at $X_{59}^{\nu^2}=-750$.

$$E_b^{\rm SO}=\frac{1}{2}[E_b(\chi_1,\chi_2)-E_b(-\chi_1,-\chi_2)], \tag{42}$$

where we have made explicit the dependence on the two dimensionless black-hole spins, χ_1 and χ_2.

Once the EOB Hamiltonian and the values of the mass ratio and spins are specified, repeating the procedure described above for different values of the frequency parameter v_ω yields the linear-in-spin binding-energy curve $E_b^{\rm SO}(v_\omega)$. Fixing $\nu=0.25$ and $\chi_1=\chi_2=0.6$, we construct such curves in both spin gauges by systematically increasing the PN order of the spin-orbit sector of the Hamiltonian, starting from the leading 1.5PN contribution and progressively including higher-order terms up to 5.5PN.[7] Since the linear-in-spin 5.5PN component of $\hat{H}_{\rm EOB}$ also depends on the unknown coefficient $X_{59}^{\nu^2}$, we vary this parameter within the range $[-750, 750]$, consistent with the $\mathcal{O}(10^2)$ estimate reported in Ref. [94].

Turning to the numerical binding-energy curve used as a reference, we rely on the data provided in Ref. [113] (see Fig. 7 therein), where the NR curves are obtained with the spectral Einstein code from numerical simulations of the simulating extreme spacetimes catalog.

The results of our analysis in both the DJS and $\overline{\text{DJS}}$ gauges are presented in Figs. 1 and 2.

In Fig. 1 we display, for both spin gauges, the binding energy obtained at different PN accuracies in the spin-orbit sector. We confirm that the DJS curves up to 4.5PN agree with those shown in Fig. 2 of Ref. [92]. Comparing the two gauges, we observe that the 1.5PN curves coincide, as expected, since spin gauge choices affect the dynamics only starting at next-to-leading order. From 2.5PN onward, each $\overline{\text{DJS}}$ curve systematically lies above the corresponding DJS one, and is therefore slightly closer to the NR binding energy.

In Fig. 2 we show a direct comparison between the 5.5PN curves obtained in the two spin gauges. We find that the $\overline{\text{DJS}}$ gauge provides a slightly better agreement with the NR data across the entire explored range of $X_{59}^{\nu^2}$ (represented by the shaded regions around the $X_{59}^{\nu^2}=0$ curve), for both positive and negative values.

It is also interesting to note that the $\overline{\text{DJS}}$ gauge exhibits a peculiar behavior at 4.5PN: its prediction is not only more accurate than the DJS curve at the same order, but even slightly more accurate than the $\overline{\text{DJS}}$ 5.5PN curve with $X_{59}^{\nu^2}=0$. Nevertheless, this 4.5PN curve lies consistently below the 5.5PN one when $X_{59}^{\nu^2}=750$ (corresponding to

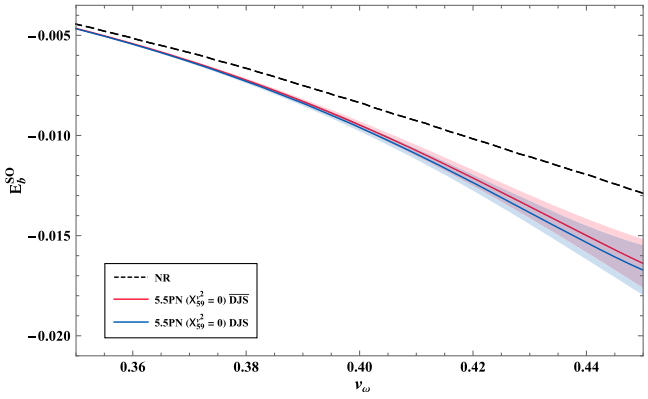

FIG. 2. Direct comparison between the 5.5PN curves shown in Fig. 1 for the two spin gauges. To better emphasize the differences between the gauges, the range of v_ω displayed here is shorter than in Fig. 1.

[7]For all PN orders below 5.5PN, we use the gauge-general expressions provided in Sec. III C of Ref. [95].

the upper edge of the pink shaded region). This observation suggests that, if one expects the 5.5PN curve to systematically improve upon the previous order, the unknown parameter $\mathsf{X}_{59}^{\nu^2}$ should take a positive and sufficiently large value.

We stress that the comparison presented here is purely qualitative in nature, as it relies on a conservative analysis in which the equations of motion are not evolved with radiation-reaction force. A quantitative assessment would require computing the EOB binding energy along a dynamical trajectory driven by dissipative effects, an analysis that goes beyond the scope of the present work.

VII. CONCLUSIONS

In this work, we have derived the gauge-general expressions for the two gyro-gravitomagnetic functions, g_S and g_{S_*}, entering the spin-orbit sector of the EOB Hamiltonian, up to 5.5PN order. Our derivation includes both local and nonlocal-in-time contributions, thereby providing a complete characterization of the spin-orbit coupling at this level of accuracy. These results extend those of previous works [93–95] either by increasing the PN accuracy or by lifting the gauge restrictions adopted therein.

We then used these expressions to compute two gauge-invariant quantities for quasicircular orbits: the binding energy and the fractional periastron advance. This constitutes a nontrivial consistency check of our gauge-general formulas, as it confirms that all dependence on the gauge coefficients cancels out when constructing physical observables.

Finally, we used our results to compare the performance of the DJS and $\overline{\text{DJS}}$ spin gauges in the specific case of an equal-mass binary with spins $\chi_1 = \chi_2 = 0.6$. This analysis is shown in Figs. 1 and 2, where we plot the spin-orbit contribution to the circular-orbit binding energy, E_b^{SO}, as a function of the frequency parameter v_ω. By comparing the analytical curves at various PN orders in the spin-orbit sector with NR data, we find that, starting at 2.5PN order, each $\overline{\text{DJS}}$ curve systematically lies slightly above the corresponding DJS curve, thereby providing a closer agreement with the NR results. Furthermore, the fact that, within the $\overline{\text{DJS}}$ gauge, the 5.5PN curve improves upon the 4.5PN one only when the undetermined coefficient $\mathsf{X}_{59}^{\nu^2}$ takes positive and sufficiently large values may be interpreted as an indication of the expected magnitude and sign of this coefficient. However, we emphasize that this comparison is purely qualitative, as radiation-reaction effects are not included in our analysis.

The main outcome of our, albeit nonconclusive, exploration is that the $\overline{\text{DJS}}$ spin gauge may offer advantages for the description of quasicircular inspirals within EOB-based waveform models. A natural direction for future work is to investigate whether the trends observed here, derived for a specific binary configuration, persist across binaries with different mass ratios and with spins of varying magnitudes and orientations.

ACKNOWLEDGMENTS

We acknowledge Marta Orselli, Marta Cocco, Elisa Grilli, and Davide Panella for many valuable discussions. G. G. and A. P. acknowledge financial support from the Italian Ministry of University and Research (MUR) through the program "Dipartimenti di Eccellenza 2023–2027" (Grant SUPER-C), from "Fondo di Ricerca d'Ateneo" 2023 (GraMB) of the University of Perugia and from the Italian Ministry of University and Research (MUR) via the PRIN 2022ZHYFA2, Gravitational waveform models for coalescing compact binaries with eccentricity (GREAT). L. S. thanks Alex Segaricci and Leonardo Dinoi for their insightful and inspiring comments during the development of this work. L. S.'s research is supported by the European Research Council (ERC) Horizon Synergy Grant "Making Sense of the Unexpected in the Gravitational-Wave Sky" Grant Agreement No. GWSky–101167314.

DATA AVAILABILITY

The data that support the findings of this article are openly available [1].

APPENDIX: QUASI-KEPLERIAN PARAMETRIZATION

The quasi-Keplerian parametrization was first introduced by Damour and Deruelle in Ref. [101], with spin contributions later included in Refs. [103,104]. Here, we review this parametrization at leading nonspinning and linear-in-spin order, which is sufficient for the computation in Sec. III. For completeness, we also refer the reader to Ref. [102] for its 3PN extension in the nonspinning case.

This parametrization is constructed to reduce, at Newtonian order, to the classical Keplerian parametrization [114], namely

$$r = a_r(1 - e\cos u_e), \tag{A1a}$$

$$\varphi - \varphi_0 = v \equiv 2\arctan\left[\left(\frac{1+e}{1-e}\right)^{1/2}\tan\frac{u_e}{2}\right], \tag{A1b}$$

$$\ell \equiv n(t - t_0) = u_e - e\sin u_e, \tag{A1c}$$

where r and φ are the usual polar coordinates in the orbital plane, with $\mathbf{r} = r(\cos\varphi, \sin\varphi, 0)$. Here, a_r denotes the semimajor axis and e is the orbital eccentricity. The auxiliary variables u_e and v are the *eccentric anomaly* and *true anomaly*, respectively. The time dependence is encoded in Kepler's equation (A1c), where ℓ is the *mean anomaly* and $n = 2\pi/T$ is the *mean motion*, with T the orbital period. The constants t_0 and φ_0 give the initial values

of the corresponding variables and can be set to zero by an appropriate choice of reference frame.

The quantities a_r, e, and n are directly related to gauge-invariant dynamical quantities—namely the μ-reduced nonrelativistic energy $\bar{E} = E - 1/\nu$ and the reduced angular momentum L—through

$$a_r = \frac{1}{-2\bar{E}}, \qquad e = \sqrt{1 + 2\bar{E}L^2}, \qquad n = (-2\bar{E})^{3/2}. \tag{A2}$$

When generalizing this parametrization to include the leading spin-orbit coupling, the above relations become [104]

$$r = a_r(1 - e_r \cos u_e), \tag{A3a}$$

$$\varphi = 2K \arctan\left[\sqrt{\frac{1+e_\varphi}{1-e_\varphi}} \tan\frac{u_e}{2}\right], \tag{A3b}$$

$$\ell \equiv nt = u_e - e_t \sin u_e, \tag{A3c}$$

where we have set $t_0 = \varphi_0 = 0$. We now have to distinguish between the three eccentricities (e_r, e_φ, e_t), i.e., the radial, angular, and time eccentricity, respectively. The factor K denotes the fractional periastron advance per radial period and encodes the precession of the orbit.

The relation between the orbital parameters and the gauge-invariant quantities can be derived from the rescaled Hamiltonian at leading nonspinning and linear-in-spin order,

$$\bar{H} = \frac{p^2}{2} - \frac{1}{r} + \frac{L}{c^3 r^3}[2\delta\chi_A - (\nu - 2)\chi_S], \tag{A4}$$

where $\bar{H} = H - c^2/\nu$ denotes the dimensionless nonrelativistic Hamiltonian. By inserting the quasi-Keplerian parametrization (A3) into Eq. (A4) and evaluating it at periastron ($u_e = 0$) and apastron ($u_e = \pi$), one obtains the relations

$$\bar{E} = -\frac{1}{2a_r} - \frac{(2-\nu)\chi_S + 2\delta\chi_A}{2c^3 a_r^{5/2}\sqrt{1-e_r^2}}, \tag{A5}$$

$$L = \sqrt{a_r(1-e_r^2)} - \frac{(e_r^2+3)[2\delta\chi_A + (2-\nu)\chi_S]}{2c^3 a_r(1-e_r^2)}. \tag{A6}$$

Inverting these equations for e_r and a_r yields

$$e_r = \sqrt{1 + 2\bar{E}L^2} + \frac{4\bar{E}(1+\bar{E}L^2)}{c^3 L\sqrt{1+2\bar{E}L^2}}[2\delta\chi_A + (2-\nu)\chi_S], \tag{A7}$$

$$a_r = \frac{-1}{2\bar{E}} + \frac{2\delta\chi_A + (2-\nu)\chi_S}{c^3 L}. \tag{A8}$$

For the mean motion and fractional periastron advance, starting from the definitions

$$T_r = \oint \frac{dr}{\dot{r}} = 2\int_{r(u_e=0)}^{r(u_e=\pi)} \frac{dr}{\partial H/\partial p_r}, \tag{A9}$$

$$K = \frac{1}{2\pi}\oint \frac{dr}{\dot{r}}\dot{\varphi} = 2\int_{r(u_e=0)}^{r(u_e=\pi)} dr \frac{\partial H/\partial L}{\partial H/\partial p_r}, \tag{A10}$$

we obtain

$$n = \frac{2\pi}{T_r} = 2\sqrt{2}(-\bar{E})^{3/2} \tag{A11}$$

$$= \frac{1}{a_r^{3/2}} + \frac{3[2\delta\chi_A + (2-\nu)\chi_S]}{2c^3 a_r^3\sqrt{1-e_t^2}}, \tag{A12}$$

$$K = 1 - \frac{2(2-\nu)\chi_S + 4\delta\chi_A}{c^3 L^3} \tag{A13}$$

$$= 1 - \frac{4\delta\chi_A + 2(2-\nu)\chi_S}{c^3 a_r^{3/2}(1-e_t^2)^{3/2}}. \tag{A14}$$

Finally, the three eccentricities are related by

$$\frac{e_r}{e_t} = 1 + \frac{2\bar{E}}{c^3 L}[2\delta\chi_A + (2-\nu)\chi_S], \tag{A15a}$$

$$\frac{e_\varphi}{e_t} = 1 + \frac{2\bar{E}}{c^3 L}[2\delta\chi_A + (2-\nu)\chi_S], \tag{A15b}$$

from which it is evident that e_r, e_φ, and e_t all coincide at leading Newtonian order. If we further substitute into Eqs. (A15a)–(A15b) the expressions for the energy and angular momentum given in Eqs. (A5)–(A6), and solve iteratively for e_t, we obtain

$$e_r = e_\varphi = e_t + \frac{e_t[(\nu-2)\chi_S - 2\delta\chi_A]}{c^3 a_r\sqrt{a_r(1-e_t^2)}}. \tag{A16}$$

[1] B. P. Abbott *et al.* (LIGO Scientific and Virgo Collaborations), Phys. Rev. X **9**, 031040 (2019).
[2] R. Abbott *et al.* (LIGO Scientific and Virgo Collaborations), Phys. Rev. X **11**, 021053 (2021).
[3] R. Abbott *et al.* (LIGO Scientific, Virgo, and KAGRA Collaborations), arXiv:2111.03606.
[4] A. H. Nitz, S. Kumar, Y.-F. Wang, S. Kastha, S. Wu, M. Schäfer, R. Dhurkunde, and C. D. Capano, Astrophys. J. **946**, 59 (2023).
[5] S. Olsen, T. Venumadhav, J. Mushkin, J. Roulet, B. Zackay, and M. Zaldarriaga, Phys. Rev. D **106**, 043009 (2022).
[6] A. G. Abac *et al.* (The LIGO Scientific, the Virgo, and the KAGRA Collaborations), arXiv:2508.18082.
[7] H. Tagoshi, A. Ohashi, and B. J. Owen, Phys. Rev. D **63**, 044006 (2001).
[8] R. A. Porto, Phys. Rev. D **73**, 104031 (2006).
[9] G. Faye, L. Blanchet, and A. Buonanno, Phys. Rev. D **74**, 104033 (2006).
[10] L. Blanchet, A. Buonanno, and G. Faye, Phys. Rev. D **74**, 104034 (2006); **75**, 049903(E) (2007); **81**, 089901(E) (2010).
[11] R. A. Porto and I. Z. Rothstein, Phys. Rev. Lett. **97**, 021101 (2006).
[12] T. Damour, P. Jaranowski, and G. Schaefer, Phys. Rev. D **77**, 064032 (2008).
[13] S. Hergt and G. Schaefer, Phys. Rev. D **78**, 124004 (2008).
[14] R. A. Porto and I. Z. Rothstein, Phys. Rev. D **78**, 044013 (2008); **81**, 029905(E) (2010).
[15] R. A. Porto and I. Z. Rothstein, Phys. Rev. D **78**, 044012 (2008); **81**, 029904(E) (2010).
[16] D. L. Perrodin, in *12th Marcel Grossmann Meeting on General Relativity* (World Scientific, Singapore, 2012), pp. 725–727.
[17] R. A. Porto, Classical Quantum Gravity **27**, 205001 (2010).
[18] S. Hergt, J. Steinhoff, and G. Schaefer, Classical Quantum Gravity **27**, 135007 (2010).
[19] L. Blanchet, A. Buonanno, and G. Faye, Phys. Rev. D **84**, 064041 (2011).
[20] J. Hartung and J. Steinhoff, Ann. Phys. (Berlin) **523**, 783 (2011).
[21] J. Hartung and J. Steinhoff, Ann. Phys. (Berlin) **523**, 919 (2011).
[22] M. Levi, Phys. Rev. D **85**, 064043 (2012).
[23] S. Marsat, A. Bohe, G. Faye, and L. Blanchet, Classical Quantum Gravity **30**, 055007 (2013).
[24] A. Bohe, S. Marsat, G. Faye, and L. Blanchet, Classical Quantum Gravity **30**, 075017 (2013).
[25] J. Hartung, J. Steinhoff, and G. Schafer, Ann. Phys. (Berlin) **525**, 359 (2013).
[26] M. Levi and J. Steinhoff, J. High Energy Phys. 06 (2015) 059.
[27] M. Levi and J. Steinhoff, J. Cosmol. Astropart. Phys. 01 (2016) 011.
[28] M. Levi and J. Steinhoff, J. Cosmol. Astropart. Phys. 01 (2016) 008.
[29] M. Levi and J. Steinhoff, J. Cosmol. Astropart. Phys. 09 (2021) 029.
[30] J. Vines and J. Steinhoff, Phys. Rev. D **97**, 064010 (2018).
[31] M. Levi, S. Mougiakakos, and M. Vieira, J. High Energy Phys. 01 (2021) 036.
[32] N. Siemonsen and J. Vines, Phys. Rev. D **101**, 064066 (2020).
[33] M. Levi, A. J. Mcleod, and M. Von Hippel, J. High Energy Phys. 07 (2021) 115.
[34] M. Levi and F. Teng, J. High Energy Phys. 01 (2021) 066.
[35] G. Cho, B. Pardo, and R. A. Porto, Phys. Rev. D **104**, 024037 (2021).
[36] Y. F. Bautista, M. Khalil, M. Sergola, C. Kavanagh, and J. Vines, Phys. Rev. D **110**, 124005 (2024).
[37] L. Blanchet, Living Rev. Relativity **17**, 2 (2014).
[38] M. Levi and J. Steinhoff, J. High Energy Phys. 09 (2015) 219.
[39] R. A. Porto, Phys. Rep. **633**, 1 (2016).
[40] M. Levi, Rep. Prog. Phys. **83**, 075901 (2020).
[41] G. Schäfer and P. Jaranowski, Living Rev. Relativity **21**, 7 (2018).
[42] K. Westpfahl and M. Goller, Lett. Nuovo Cimento **26**, 573 (1979).
[43] L. Bel, T. Damour, N. Deruelle, J. Ibanez, and J. Martin, Gen. Relativ. Gravit. **13**, 963 (1981).
[44] T. Damour, Phys. Rev. D **94**, 104015 (2016).
[45] T. Damour, Phys. Rev. D **97**, 044038 (2018).
[46] Y. Mino, M. Sasaki, and T. Tanaka, Phys. Rev. D **55**, 3457 (1997).
[47] T. C. Quinn and R. M. Wald, Phys. Rev. D **56**, 3381 (1997).
[48] L. Barack and A. Pound, Rep. Prog. Phys. **82**, 016904 (2019).
[49] A. Pound and B. Wardell, Black hole perturbation theory and gravitational self-force, in *Handbook of Gravitational Wave Astronomy* (Springer, Singapore, 2021).
[50] A. Buonanno and T. Damour, Phys. Rev. D **62**, 064015 (2000).
[51] T. Damour, P. Jaranowski, and G. Schaefer, Phys. Rev. D **62**, 084011 (2000).
[52] T. Damour, Phys. Rev. D **64**, 124013 (2001).
[53] T. Damour, P. Jaranowski, and G. Schäfer, Phys. Rev. D **91**, 084024 (2015).
[54] S. Akcay, R. Gamba, and S. Bernuzzi, Phys. Rev. D **103**, 024014 (2021).
[55] S. Schmidt, M. Breschi, R. Gamba, G. Pagano, P. Rettegno, G. Riemenschneider, S. Bernuzzi, A. Nagar, and W. Del Pozzo, Phys. Rev. D **103**, 043020 (2021).
[56] A. Nagar, P. Rettegno, R. Gamba, and S. Bernuzzi, Phys. Rev. D **103**, 064013 (2021).
[57] S. Ossokine *et al.*, Phys. Rev. D **102**, 044055 (2020).
[58] D. A. Godzieba, R. Gamba, D. Radice, and S. Bernuzzi, Phys. Rev. D **103**, 063036 (2021).
[59] R. Gamba, S. Bernuzzi, and A. Nagar, Phys. Rev. D **104**, 084058 (2021).
[60] R. Gamba, M. Breschi, S. Bernuzzi, M. Agathos, and A. Nagar, Phys. Rev. D **103**, 124015 (2021).
[61] A. Matas *et al.*, Phys. Rev. D **102**, 043023 (2020).
[62] G. Riemenschneider, P. Rettegno, M. Breschi, A. Albertini, R. Gamba, S. Bernuzzi, and A. Nagar, Phys. Rev. D **104**, 104045 (2021).
[63] R. Gamba, S. Akçay, S. Bernuzzi, and J. Williams, Phys. Rev. D **106**, 024020 (2022).

[64] R. Gamba, M. Breschi, G. Carullo, P. Rettegno, S. Albanesi, S. Bernuzzi, and A. Nagar, Nat. Astron. **7**, 11 (2023).
[65] A. Ramos-Buades, A. Buonanno, M. Khalil, and S. Ossokine, Phys. Rev. D **105**, 044035 (2022).
[66] A. Bonino, R. Gamba, P. Schmidt, A. Nagar, G. Pratten, M. Breschi, P. Rettegno, and S. Bernuzzi, Phys. Rev. D **107**, 064024 (2023).
[67] A. Placidi, S. Albanesi, A. Nagar, M. Orselli, S. Bernuzzi, and G. Grignani, Phys. Rev. D **105**, 104030 (2022).
[68] S. Albanesi, A. Placidi, A. Nagar, M. Orselli, and S. Bernuzzi, Phys. Rev. D **105**, L121503 (2022).
[69] A. Gonzalez, R. Gamba, M. Breschi, F. Zappa, G. Carullo, S. Bernuzzi, and A. Nagar, Phys. Rev. D **107**, 084026 (2023).
[70] A. Placidi, G. Grignani, T. Harmark, M. Orselli, S. Gliorio, and A. Nagar, Phys. Rev. D **108**, 024068 (2023).
[71] S. Albanesi, S. Bernuzzi, T. Damour, A. Nagar, and A. Placidi, Phys. Rev. D **108**, 084037 (2023).
[72] E. Grilli, A. Placidi, S. Albanesi, G. Grignani, and M. Orselli, Phys. Rev. D **111**, 044045 (2025).
[73] A. Nagar, D. Chiaramello, R. Gamba, S. Albanesi, S. Bernuzzi, V. Fantini, M. Panzeri, and P. Rettegno, Phys. Rev. D **111**, 064050 (2025).
[74] T. Damour, A. Nagar, A. Placidi, and P. Rettegno, Phys. Rev. D **113**, 024042 (2026).
[75] S. Albanesi, R. Gamba, S. Bernuzzi, J. Fontbuté, A. Gonzalez, and A. Nagar, Phys. Rev. D **112**, L121503 (2025).
[76] L. Nagni, A. Nagar, R. Gamba, S. Albanesi, and S. Bernuzzi, Phys. Rev. D **113**, 044052 (2026).
[77] L. Pompili *et al.*, Phys. Rev. D **108**, 124035 (2023).
[78] M. van de Meent, A. Buonanno, D. P. Mihaylov, S. Ossokine, L. Pompili, N. Warburton, A. Pound, B. Wardell, L. Durkan, and J. Miller, Phys. Rev. D **108**, 124038 (2023).
[79] A. Gamboa, M. Khalil, and A. Buonanno, Phys. Rev. D **112**, 044037 (2025).
[80] A. Gamboa, A. Buonanno, R. Enficiaud, M. Khalil, A. Ramos-Buades, L. Pompili, H. Estellés, M. Boyle, L. E. Kidder, H. P. Pfeiffer *et al.*, Phys. Rev. D **112**, 044038 (2025).
[81] A. Ramos-Buades, A. Buonanno, H. Estellés, M. Khalil, D. P. Mihaylov, S. Ossokine, L. Pompili, and M. Shiferaw, Phys. Rev. D **108**, 124037 (2023).
[82] T. Damour, P. Jaranowski, and G. Schäfer, Phys. Rev. D **78**, 024009 (2008).
[83] A. Buonanno, G. Mogull, R. Patil, and L. Pompili, Phys. Rev. Lett. **133**, 211402 (2024).
[84] A. Nagar, Phys. Rev. D **84**, 084028 (2011).
[85] E. Barausse and A. Buonanno, Phys. Rev. D **84**, 104027 (2011).
[86] M. K. Mandal, P. Mastrolia, R. Patil, and J. Steinhoff, J. High Energy Phys. 03 (2023) 130.
[87] J.-W. Kim, M. Levi, and Z. Yin, J. High Energy Phys. 05 (2023) 184.
[88] D. Bini, T. Damour, and A. Geralico, Phys. Rev. Lett. **123**, 231104 (2019).
[89] D. Bini, T. Damour, and A. Geralico, Phys. Rev. D **102**, 024062 (2020).
[90] D. Bini, T. Damour, and A. Geralico, Phys. Rev. D **102**, 024061 (2020).
[91] D. Bini, T. Damour, and A. Geralico, Phys. Rev. D **102**, 084047 (2020).
[92] A. Antonelli, C. Kavanagh, M. Khalil, J. Steinhoff, and J. Vines, Phys. Rev. Lett. **125**, 011103 (2020).
[93] A. Antonelli, C. Kavanagh, M. Khalil, J. Steinhoff, and J. Vines, Phys. Rev. D **102**, 124024 (2020).
[94] M. Khalil, Phys. Rev. D **104**, 124015 (2021).
[95] A. Placidi, P. Rettegno, and A. Nagar, Phys. Rev. D **109**, 084065 (2024).
[96] A. Albertini, A. Nagar, J. Mathews, and G. Lukes-Gerakopoulos, Phys. Rev. D **110**, 044034 (2024).
[97] See Supplemental Materials at http://link.aps.org/supplemental/10.1103/435y-8241 that accompanies this paper for the electronic form of all the main analytical results derived throughout it.
[98] L. Blanchet and G. Faye, J. Math. Phys. (N.Y.) **41**, 7675 (2000).
[99] L. Blanchet and T. Damour, Ann. l'I. H. P. Phys. Théor. **50**, 377 (1989).
[100] L. E. Kidder, Phys. Rev. D **52**, 821 (1995).
[101] T. Damour and N. Deruelle, Ann. l'I.H.P. Phys. Théor. **43**, 107 (1985).
[102] R.-M. Memmesheimer, A. Gopakumar, and G. Schäfer, Phys. Rev. D **70**, 104011 (2004).
[103] M. Tessmer, J. Hartung, and G. Schäfer, Classical Quantum Gravity **27**, 165005 (2010).
[104] M. Tessmer, J. Hartung, and G. Schäfer, Classical Quantum Gravity **30**, 015007 (2012).
[105] T. Damour and N. Deruelle, Ann. l'I.H.P. Phys. Théor. **44**, 263 (1986).
[106] T. Damour, P. Jaranowski, and G. Schäfer, Phys. Rev. D **89**, 064058 (2014).
[107] T. Damour, Phys. Rev. D **94**, 104015 (2016).
[108] T. Damour, Phys. Rev. D **97**, 044038 (2018).
[109] T. Hinderer, A. Buonanno, A. H. Mroué, D. A. Hemberger, G. Lovelace, H. P. Pfeiffer, L. E. Kidder, M. A. Scheel, B. Szilagyi, N. W. Taylor *et al.*, Phys. Rev. D **88**, 084005 (2013).
[110] T. Damour and A. Nagar, Phys. Rev. D **90**, 044018 (2014).
[111] P. Rettegno, F. Martinetti, A. Nagar, D. Bini, G. Riemenschneider, and T. Damour, Phys. Rev. D **101**, 104027 (2020).
[112] D. Bini, T. Damour, and A. Geralico, Phys. Rev. D **92**, 124058 (2015); **93**, 109902(E) (2016).
[113] S. Ossokine, T. Dietrich, E. Foley, R. Katebi, and G. Lovelace, Phys. Rev. D **98**, 104057 (2018).
[114] D. Brouwer and G. M. Clemence, *Methods of Celestial Mechanics* (Academic Press, New York, 1961).